Provided for non-commercial research and education use.
Not for reproduction, distribution or commercial use.

This article appeared in a journal published by Elsevier. The attached copy is furnished to the author for internal non-commercial research and education use, including for instruction at the authors institution and sharing with colleagues.

Other uses, including reproduction and distribution, or selling or licensing copies, or posting to personal, institutional or third party websites are prohibited.

In most cases authors are permitted to post their version of the article (e.g. in Word or Tex form) to their personal website or institutional repository. Authors requiring further information regarding Elsevier's archiving and manuscript policies are encouraged to visit:

http://www.elsevier.com/copyright

Author's personal copy

FUNGAL BIOLOGY REVIEWS 25 (2011) 14–37

ELSEVIER

British Mycological Society promoting fungal science

journal homepage: www.elsevier.com/locate/fbr

Plenary Paper

The dynamic fungal cell

Gero STEINBERG[a,*], *Martin SCHUSTER*[b]

[a]*Department of Biosciences, University of Exeter, Exeter EX4 4QD, UK*
[b]*Bioimaging Centre, University of Exeter, Exeter EX4 4QD, UK*

ARTICLE INFO

Article history:
Received 12 January 2011
Received in revised form
18 January 2011
Accepted 20 January 2011

Keywords:
Cytoskeleton
Dynamic
F-actin
Fungal cell
Microtubules: Movie clips
Organelle motility

ABSTRACT

Filamentous fungi are fascinating organisms that combine technical amenability with interesting biology and economical and ecological importance. In recent years, intensive research has rapidly extended our knowledge in many of the sub-disciplines in fungal sciences. An upcoming challenge is the integration of this detailed information in a more holistic understanding of the organisation and function of the fungal cell and its interaction with the environment. Here we provide an extensive visual impression of the organisation and motility of cellular structures in hyphae and yeast-like cells of the corn pathogen *Ustilago maydis*. We show 3D animation of major cytoskeletal elements and organelles in yeast-like and hyphal cells and provide insight into their dynamic behaviour. Using laser-based epi-fluorescence, we also include some more specialised processes, such as the dynamics of microtubules in mitosis, F-actin patches turn-over during endocytic uptake, nuclear import in interphase and in late mitosis and diffusion within the endoplasmic reticulum and the plasma membrane. This collection of 76 previously unpublished movie clips should provide a useful source for teaching fungal cell biology, but also intends to inspire researchers in different areas of fungal science.

© 2011 The British Mycological Society. Published by Elsevier Ltd. All rights reserved.

Introduction

Molecular cell biology is a rapidly progressing field in fungal research. Since Robert Hook defined the term "cell" in the 17th century by observing cork using a simple microscope (Hooke, 1665), cell biology has been a visual discipline and microscopy a central technique. In the 19th century cell biological studies demonstrated that filamentous fungi can cause animal, human and plant diseases (Bristowe, 1854; Kühn, 1858; overview in Hallmann *et al.*, 2010; Hinson *et al.*, 1952). Since then applied aspect is still in focus, but more fundamental questions, such as the cellular basis of hyphal growth, have attracted scientist from the early days on (Reinhardt, 1892; Brunswik, 1924). Today, we have a much clearer understanding of the biology of fungal infection (for further reading see Nielsen and Heitman, 2007; van de Veerdonk *et al.*, 2008; Wilson and Talbot, 2009; Brefort *et al.*, 2009; Skamnioti and Gurr, 2009; Seider *et al.*, 2010; Mehrabi *et al.*, 2011), and a powerful combination of molecular genetics and live cell imaging has provided insight into the molecular basis of fungal morphogenesis, cellular function and hyphal growth (for further reading see Oakley, 2004; Sudbery *et al.*, 2004; Harris *et al.*, 2005; Steinberg, 2007a; Latge, 2007; De Souza and Osmani, 2007; Fischer *et al.*, 2008; Veses *et al.*, 2008; Brand and Gow, 2009; Read *et al.*, 2009; Gladfelter, 2010; Penalva, 2010; Maerz and Seiler, 2010; Zarnack and Feldbrügge, 2010).

In this article we set out to give a visual impression of the organisation and motility of cellular structures in a fungal cell. We have used fluorescent marker proteins and labelled subcellular structures and compartments in the yeast-like and hyphal cells of the plant pathogen *Ustilago maydis* (Fig. 1; for

* Tel.: +44 1392 263476; fax: +44 1392 263434.
Abbreviations: EE, early endosomes; ER, endoplasmic reticulum; GFP, green fluorescent protein; RFP, red fluorescent protein.
E-mail address: G.Steinberg@exeter.ac.uk (G. Steinberg).
1749-4613/$ – see front matter © 2011 The British Mycological Society. Published by Elsevier Ltd. All rights reserved.
doi:10.1016/j.fbr.2011.01.008

Author's personal copy

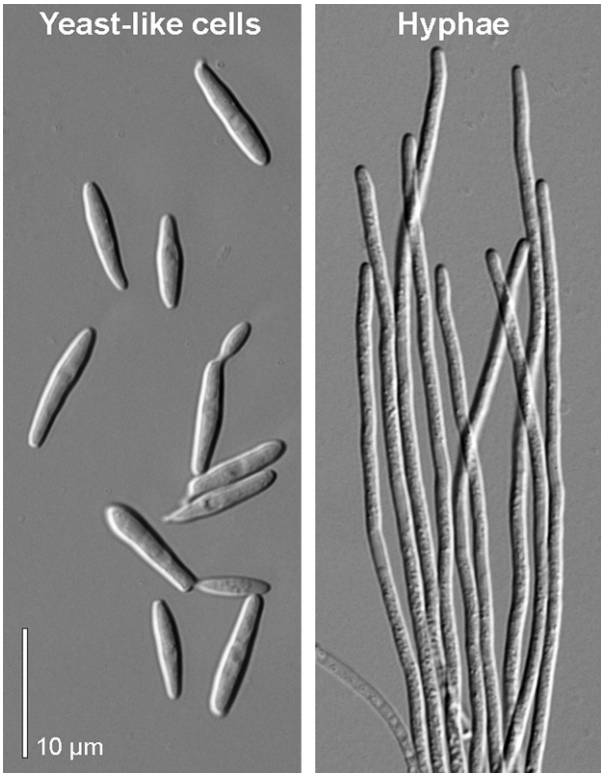

Fig. 1 – The dimorphic fungus *U. maydis*. The corn smut fungus is a pathogen on *Zea maize*. In rich media it grows as a budding yeast-like cell (Bölker, 2001; Brefort *et al.*, 2009). Upon recognition of a mating partner the fungus switches to hyphal growth and invades the host tissue (Brachmann *et al.*, 2001; Spellig *et al.*, 1994). The hyphal form is induced and maintained due to the activity of the *b*-transcription factor (Schulz *et al.*, 1990; Kämper *et al.*, 1995; Kahmann *et al.*, 1995). The bar represents 10 μm.

further reading about this model fungus see Banuett, 1995; Bölker, 2001; Perez-Martin *et al.*, 2006; Steinberg and Perez-Martin, 2008; Brefort *et al.*, 2009). We provide a collection of new movies that illustrate the 3-dimensional organisation and the dynamic behaviour of the cytoskeleton and major compartments in these fungal cells. The movies can be accessed by clicking on the thumbnails in the section following the introduction. Alternatively, the movies (in WMF and FLV [Windows], and MP4 and MOV [MAC] format) can be downloaded from ScienceDirect (doi:10.1016/j.fbr.2011.01.008) or are included in the DVD accompanying the printed issue. In addition, this DVD contains a supplementary PowerPoint presentation and larger AVI movies (in the AVI folder). This provides easy access to all movies and allows the reader to copy the annotated movies into existing presentations (please note that the presentation does have to be in the same folder as the AVI movies).

We start the journey through the cell with the cytoskeleton. Tubulin and actin assemble into protein fibres, which are known as microtubules and filamentous actin (F-actin). Both are of central importance for organelle motility and organisation (Xiang and Fischer, 2004; Steinberg, 2007a,b; Fischer *et al.*, 2008). Our movie collection therefore starts with microtubules (Movies 1–12), which are required for continuous filamentous growth of fungi (Horio and Oakley, 2005; Fuchs *et al.*, 2005). Interphase microtubules are seen in Movies 1–5. In mitosis the spindle forms long astral microtubules (Movies 6–8). Cortical interaction of these astral microtubules exerts force on the mitotic spindle (Steinberg *et al.*, 2001; Fink *et al.*, 2006), which is documented in Movies 9–12. The second major cytoskeletal element is filamentous actin. A crucial role for actin in hyphal growth is well established (Heath, 1995; Heath and Steinberg, 1999; Heath *et al.*, 2000; Fuchs *et al.*, 2005). Peripheral actin patches mark sites of endocytosis and their continuous turnover support endocytosis (Kaksonen *et al.*, 2003; Rodal *et al.*, 2005). In addition, F-actin forms long tracks (Berepiki *et al.*, 2010; Delgado-Alvarez *et al.*, 2010) that might support myosin motor motility. We show the organisation and dynamics of F-actin in Movies 13–18. Motor proteins (Fig. 2) use the fibres of the cytoskeleton to transport cargo through the cell (Xiang and Plamann, 2003; Vale, 2003). The major transporters for vesicles and organelles in filamentous fungi are myosin-5 (Woo *et al.*, 2003; Weber *et al.*, 2003), kinesin-3 (Wedlich-Söldner *et al.*, 2002a; Lenz *et al.*, 2006; Zekert and Fischer, 2009) and dynein (Plamann *et al.*, 1994; Xiang *et al.*, 1994; Straube *et al.*, 2001; Alberti-Segui *et al.*, 2001; Martin *et al.*, 2004). By improving our microscopic setup and using laser-based epi-fluorescence (see Methods for details) we succeeded in visualising the motility of single motors in living hyphal cells (Schuster *et al.*, 2011 (a,b)). This allowed quantitative analysis and mathematical modelling approaches (Schuster *et al.*, 2011(a); Ashwin *et al.*, 2010). We give examples of motor behaviour in *U. maydis* in Movies 19–24. Kinesin-3 and dynein mediate early endosomes motility (Wedlich-Söldner *et al.*, 2002a; Lenz *et al.*, 2006; Zhang *et al.*, 2010), which is in focus in the following video clips (Movies 25–31). Movie 30 is a nice example of endosomes moving along microtubules and Movie 31 demonstrates co-localisation of early endosomes and kinesin-3. Early endosomes are thought to have a dual role in sorting to the vacuole (Movies 32–36) and recycling back to the plasma membrane (Movie 37). According to the "fluid mosaic model" (Singer and Nicolson, 1972), the proteins can diffuse in the plasma membrane. This is nicely seen in fluorescence recovery after photo-bleaching (FRAP) experiments (Movies 38).

Fungal hyphae concentrate sphingolipids at the hyphal tip (Martin and Konopka, 2004; Canovas and Perez-Martin, 2009; overview in Steinberg, 2007a). This reduces fluidity of the membrane, and is expected to impair protein diffusion at the hyphal tip. The differences in membrane fluidity between subapical regions and the apex can be seen in Movies 38 and 39. The plasma membrane receives secretory vesicles containing proteins that travel from the endoplasmic reticulum *via* the Golgi apparatus to the surface. Movies that show the organisation and dynamic behaviour of the endoplasmic reticulum (Movies 40–47) and the Golgi apparatus (Movies 48–53) are part of the provided collection. An important class of secretory vesicles are chitosomes that are characterised by the presence of membrane-bound chitin synthase (Sietsma *et al.*, 1996; Bartnicki-Garcia, 2006; Riquelme *et al.*, 2007; Movie 54). Using photo-bleaching techniques the motility of chitin synthase 8, a class V chitin synthase, was visualised (Treitschke *et al.*, 2010; Movie 55). Class V chitin synthases contain a myosin motor domain and are considered to be able to participate in transport of their attached chitosome

Author's personal copy

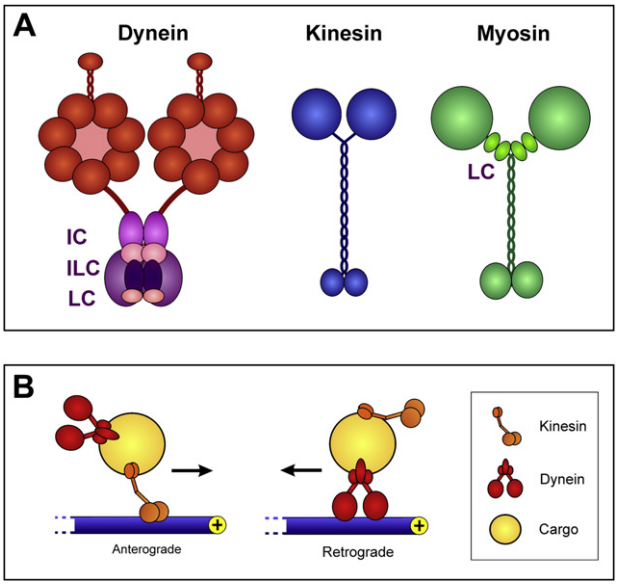

Fig. 2 – Molecular motors. (A) The organisation of molecular motors. All motors consist of heavy chains (HC) that form the motor domain (Motor) and in many cases bind light chains (LC). The dynein complex contains additional intermediate chains (IC) and intermediate light chains (ILC). Note that kinesin-1 and myosin-5 are shown. The organisation of kinesins and myosins belonging to different classes might vary (Vale, 2003). (B) Model of motor cooperation in long-range transport along microtubules. Motors carry their cargo (e.g. an organelle) to the plus- or the minus end. The opposing motor can be a passive cargo, thereby getting recycled for another round of transport. Note that transport of early endosomes in *U. maydis* differs in that dynein is not a passive cargo of the organelles (Schuster *et al.* 2011(b)).

(Fujiwara *et al.*, 1997; Madrid *et al.*, 2003; Abramczyk *et al.*, 2009). However, the motor domain is not required for chitin synthase 8 motility in *U. maydis* (Treitschke *et al.*, 2010; Movie 56). The endoplasmic reticulum forms a continuum with the nuclear envelope and contains proteins that contain a nuclear localisation signal (Movies 59–63). This signal mediates active import through highly specialised nuclear pores (De Souza *et al.*, 2004; Osmani *et al.*, 2006; Theisen *et al.*, 2008; Movie 64). This occurs in interphase cells and is visible after photo-bleaching of imported nuclear GFP (Movie 65). Nuclear import is also important to reconstitute the nucleus after mitosis when the nuclear envelope gets removed (Straube *et al.*, 2005) or is partially permeable due to a disassembly of the pores (De Souza and Osmani, 2007). Reimport after "open mitosis" in *U. maydis* can be observed in Movie 65. Finally, we have included movies showing peroxisomes (Movies 67–71) and mitochondria (Movies 72–76). In fungi both organelles are dynamic (van der Klei and Veenhuis, 2002; Westermann and Prokisch, 2002; Fuchs and Westermann, 2005). Mitochondria provide the metabolic "fuel" to drive molecular processes, and fungal peroxisomes function in lipid metabolism and detoxification (Schrader and Fahimi, 2008). In addition, peroxisomes serve additional functions in penicillin biosynthesis (Kiel *et al.*, 2000; Sprote *et al.*, 2009) and indirectly support microtubule nucleation (Zekert *et al.*, 2010). The movie collection represents the status of our current understanding in *U. maydis*, and it is important to realise that the sub-cellular organisation most likely varies between fungal species. However, most of the basic organising principles and mechanisms are expected to be conserved.

Microtubules

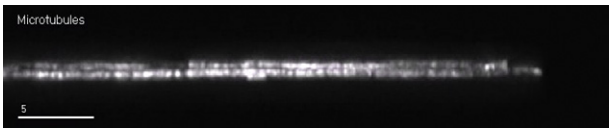

Movie 1 Microtubule organisation in a hyphal cell. Microtubules form bundles that extend from the growing tip to the proximal septum, thereby providing continuous tracks that connect both cell poles. Note that individual microtubules can be very short and are not nucleated at the spindle pole body, a nuclear microtubule organising centre. Microtubules were visualised by eGFP fused to the alpha-tubulin gene *tub1* (Steinberg *et al.*, 2001). The 3D reconstruction was built from a deconvolved Z-axis image stack. The bar represents 5 μm. Click here or on image to access the movie.

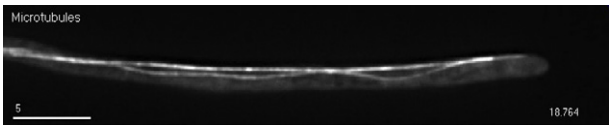

Movie 2 Microtubule dynamics in a hyphal cell. Single microtubule undergoes frequent bending and waving whereas the bundles are less flexible. The movie was built from a deconvolved image series. Microtubules were visualised by eGFP fused to the alpha-tubulin gene *tub1* (Steinberg *et al.*, 2001). The time is given in seconds and milliseconds, the bar represents 5 μm. Click here or on image to access the movie.

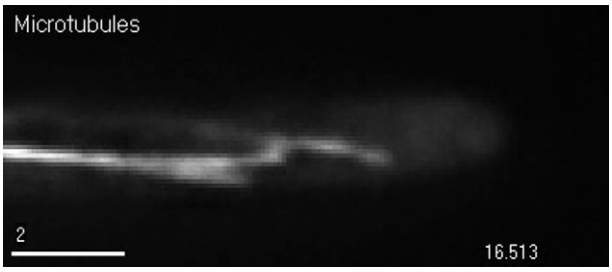

Movie 3 Microtubule dynamics at the growing tip of a hyphal cell. Microtubules grow by polymerisation of their subunits and shrink by depolymerisation. In addition, microtubule motility adds to the microtubule dynamic behaviour. Note that the microtubules do not reach into the hyphal apex. Microtubules were visualised by eGFP fused to the alpha-tubulin gene *tub1* (Steinberg *et al.*, 2001). The movie was built from a deconvolved image series. The time is given in seconds: milliseconds; the bar represents 2 μm. Click here or on image to access the movie.

Author's personal copy

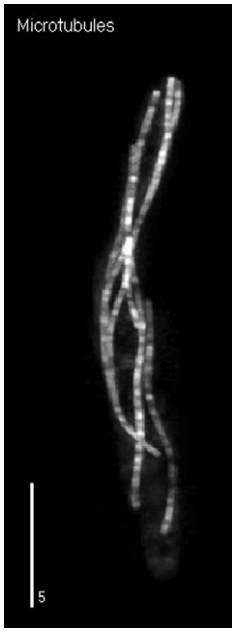

Microtubule dynamics in a hyphal cell. Single microtubule undergoes frequent bending and waving whereas the bundles are less flexible. The movie was built from a deconvolved image series. Microtubules were visualised

Movie 4 Microtubule organisation in a yeast-like cell. Microtubules connect the growth region (top) with the mother cell (bottom). Microtubules have a tendency to form bundles and the microtubule array connects the cell poles. Like in hyphal cells, individual microtubules can be very short and are not nucleated at the spindle pole body, but are formed at cytoplasmic sites near the bud neck (Straube *et al.*, 2003; Fink and Steinberg, 2006). Microtubules were visualised by eGFP fused to the alpha-tubulin gene *tub1* (Steinberg *et al.*, 2001). The 3D reconstruction was built from a deconvolved Z-axis image stack. The bar represents 5 μm. Click here or on image to access the movie.

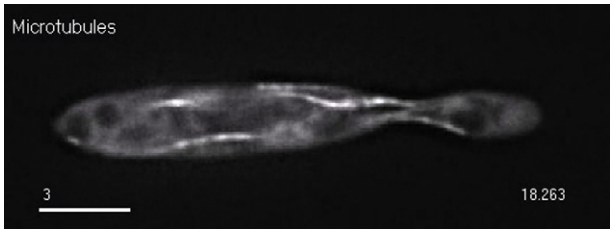

Movie 5 Microtubule dynamics in a yeast-like cell. Single microtubules polymerise and depolymerise. Dark patches on the microtubules (regions of less fluorescence called "speckles"), can serve as "landmarks" that demonstrate that (a) microtubules indeed elongate and (b) undergo short range to-and-fro motion. Microtubules were visualised by eGFP fused to the alpha-tubulin gene *tub1* (Steinberg *et al.*, 2001). The movie was built from a deconvolved image series. The time is given in seconds: milliseconds; the bar represents 3 μm. Click here or on image to access the movie.

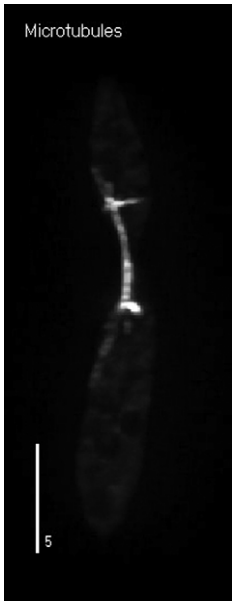

Microtubule organisation in a mitotic cell during phase. The anaphase spindle is positioned in the and a few astral microtubules extend into the nd the daughter cell. The chromosomes are located very closely to the spindle pole bodies (not visible). Microtubules were visualised by eGFP fused to the alpha-tubulin gene *tub1* (Steinberg *et al.*, 2001). The 3D reconstruction was built from a deconvolved Z-axis image stack. The bar represents 5 μm. Click here or on image to access the movie.

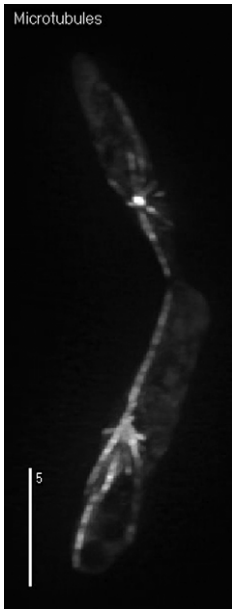

Movie 7 Microtubule organisation in a mitotic cell during late anaphase. The anaphase spindle extends from the daughter to the mother cell. Numerous astral microtubules are formed that position both spindle poles in the cell centres. Microtubules were visualised by eGFP fused to the alpha-tubulin gene *tub1* (Steinberg *et al.*, 2001). The 3D reconstruction was built from a deconvolved Z-axis image stack. The bar represents 5 μm. Click here or on image to access the movie.

Author's personal copy

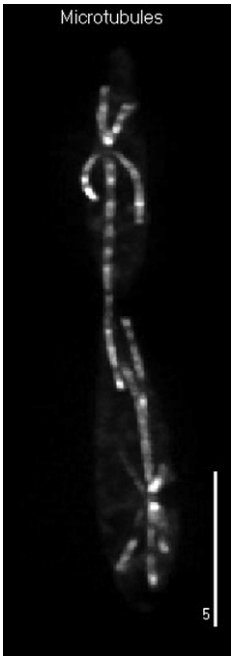

Movie 8 Microtubule organisation in a mitotic cell in telophase. Both spindle poles and the attached chromosomes (not visible) are positioned in the mother and the daughter cell. The astral microtubules keep them in position. The central spindle is disrupted. Note that at this stage chromosomes de-condense and the nuclear envelopes reappear (Straube *et al.*, 2005). The anaphase spindle extends from the daughter to the mother cell. Microtubules were visualised by eGFP fused to the alpha-tubulin gene *tub1* (Steinberg *et al.*, 2001). The 3D reconstruction was built from a deconvolved Z-axis image stack. The bar represents 3 μm. Click here or on image to access the movie.

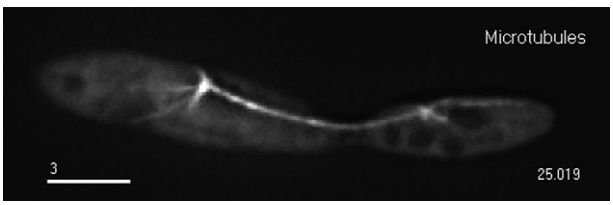

Movies 9 and 10 Microtubule dynamics in a mitotic cell during anaphase. Long astral microtubules emanate from the spindle pole bodies and contact the cell cortex (cell periphery). Here cytoplasmic dynein pulls on the astral microtubules thereby elongating the spindle. The chromosomes (not visible) are located very close to the spindle pole bodies. Note that the behaviour of the spindle indicates counteracting forces exerted at both sides of the spindle. Movie 9 provides extended annotation in the first movie frame. Microtubules were visualised by eGFP fused to the alpha-tubulin gene *tub1* (Steinberg *et al.*, 2001). The movie was built from a deconvolved image series. The time is given in seconds: milliseconds; the bar represents 3 μm.Click here or on image to access the movie.

Movie 11 Microtubule dynamics in a mitotic cell during anaphase. This second example shows rapid spindle elongation during anaphase. Long astral microtubules emanate from the spindle pole bodies and contact the cell cortex. Their interaction with dynein that is stationary at the cell periphery drives the elongation of the spindle. Note the to-and-fro motion of the spindle, indicating counteracting forces. Microtubules were visualised by eGFP fused to the alpha-tubulin gene *tub1* (Steinberg *et al.*, 2001). The movie was built from a deconvolved image series. The time is given in seconds: milliseconds; the bar represents 5 μm. Click here or on image to access the movie.

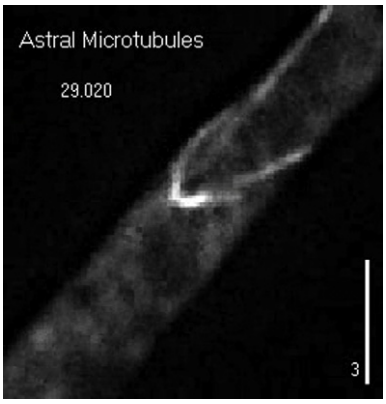

Movie 12 Dynamics of a microtubule aster during anaphase. The movie demonstrates the dynamic behaviour of the astral microtubules. Their interaction with dynein at the cellular cortex drives the motility of the

Author's personal copy

spindle pole and thereby the segregation of the chromosomes (Fink *et al.*, 2006). Microtubules were visualised by eGFP fused to the alpha-tubulin gene *tub1* (Steinberg *et al.*, 2001). The movie was built from a deconvolved image series. The time is given in seconds: milliseconds; the bar represents 3 μm. Click here or on image to access the movie.

Filamentous actin (F-actin)

Movie 13 F-actin organisation in a hyphal cell. F-actin is found as long peripheral filaments and brightly labelled peripheral patches. The cables provide "tracks" for myosin motors, whereas the patches represent unordered F-actin accumulations that, due to their capacity to polymerise, are thought to propel endocytic vesicles from the cell periphery into the cytoplasm (Rodal *et al.*, 2005). Actin patches are concentrated at the hyphal tip indicating that this region is active in endocytosis. F-actin was visualised by eGFP fused to a Lifeact-peptide (Schuster, submitted for publication). The Lifeact-peptide was developed in the budding yeast (Riedl *et al.*, 2008) and was used to visualise F-actin in *Neurospora crassa* (Berepiki *et al.*, 2010; Delgado-Alvarez *et al.*, 2010). The 3D reconstruction was built from a deconvolved Z-axis image stack. The bar represents 5 μm. Click here or on image to access the movie.

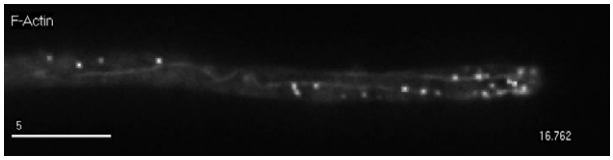

Movie 14 Dynamics of F-actin in the periphery of a hyphal cell. Actin patches are continuously formed at the cell periphery and are rapidly disappearing, which indicates that (a) they leave the focal plane by pushing themselves into the cytoplasm and (b) they disassemble shortly after leaving the plasma membrane. Note that actin "cables" are reaching into the hyphal apex. F-actin was visualised by eGFP fused to a Lifeact-peptide (Schuster, submitted for publication). The Lifeact-peptide was developed in the budding yeast (Riedl *et al.*, 2008) and was used to visualise F-actin in *N. crassa* (Berepiki *et al.*, 2010; Delgado-Alvarez *et al.*, 2010). The movie was built from a deconvolved image series. The time is given in seconds: milliseconds; the bar represents 5 μm. Click here or on image to access the movie.

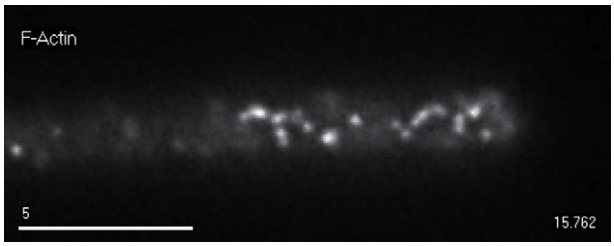

Movie 15 Dynamics of F-actin patches at the tip of a hyphal cell. Actin patches are continuously formed at the cell periphery and are rapidly disappearing due to their disassembly and their motility out of the focal plane. F-actin was visualised by eGFP fused to a Lifeact-peptide (Schuster, submitted for publication). The Lifeact-peptide was developed in the budding yeast (Riedl *et al.*, 2008) and was used to visualise F-actin in *N. crassa* (Berepiki *et al.*, 2010; Delgado-Alvarez *et al.*, 2010). The movie was built from a deconvolved image series. The time is given in seconds: milliseconds; the bar represents 3 μm. Click here or on image to access the movie.

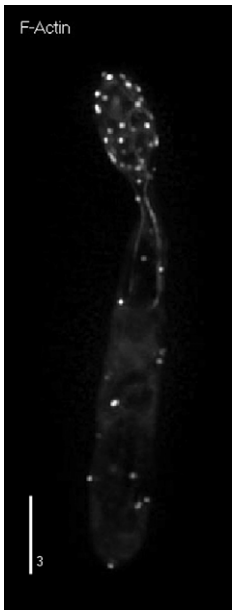

Movie 16 F-actin organisation in a yeast-like cell. F-actin forms peripheral filaments that connect the bud with the mother cell. In addition, brightly labelled peripheral patches are visible that concentrated at the growth region where endocytosis occurs. F-actin was visualised by eGFP fused to a Lifeact-peptide (Schuster, submitted for publication). The Lifeact-peptide was developed in the budding yeast (Riedl *et al.*, 2008) and was used to visualise F-actin in *N. crassa* (Berepiki *et al.*, 2010; Delgado-Alvarez *et al.*, 2010). The 3D reconstruction was built from a deconvolved Z-axis image stack. The bar represents 3 μm. Click here or on image to access the movie.

Author's personal copy

Movie 17 Dynamics of F-actin in a yeast-like cell. Actin patches are transiently visible. Note that the cables are stable peripheral structures. Patches occasionally move over some distances, indicating the motility of endocytic vesicles that are propelled by actin polymerisation. F-actin was visualised by eGFP fused to a Lifeact-peptide (Schuster, submitted for publication). The Lifeact-peptide was developed in the budding yeast (Riedl *et al.*, 2008) and was used to visualise F-actin in *N. crassa* (Berepiki *et al.*, 2010; Delgado-Alvarez *et al.*, 2010). The movie was built from a deconvolved image series. The time is given in seconds: milliseconds; the bar represents 3 μm. Click here or on image to access the movie.

Movie 18 Dynamics of F-actin patches in the bud of yeast-like cell. Actin patches are continuously formed at the cell periphery and are rapidly disappearing due to their disassembly and their motility out of the focal plane. In addition, some patches show short range movement. Note that the movie was taken at a medial focal plane. Consequently, most patches are found at the cell edge near the plasma membrane. In addition, few patches are found in the cytoplasm. F-actin was visualised by eGFP fused to a Lifeact-peptide (Schuster, submitted for publication). The Lifeact-peptide was developed in the budding yeast (Riedl *et al.*, 2008) and was used to visualise F-actin in *N. crassa* (Berepiki *et al.*, 2010; Delgado-Alvarez *et al.*, 2010). The movie was built from a deconvolved image series. The time is given in seconds: milliseconds; the bar represents 2 μm. Click here or on image to access the movie.

Molecular motors

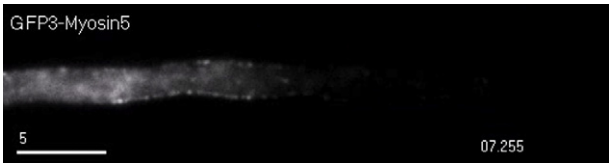

Movie 19 Dynamics of myosin-5 in a hyphal cell. Expression of GFP_3-myosin-5 generates a strong cytoplasmic background which interferes with the specific signals. Pre-treatment with a 405 nm laser photo-bleaches the cell (indicated by red box and "Bleach"), allowing the observation of myosin-5 motors moving towards the hyphal tip. myosin-5 was labelled by fusing a triple GFP tag to the N-terminus of the *myo*5 gene (Weber *et al.*, 2003). The construct is integrated in the native locus; therefore native levels of the motors are shown. The time is given in seconds: milliseconds; the bar represents 5 μm. Click here or on image to access the movie.

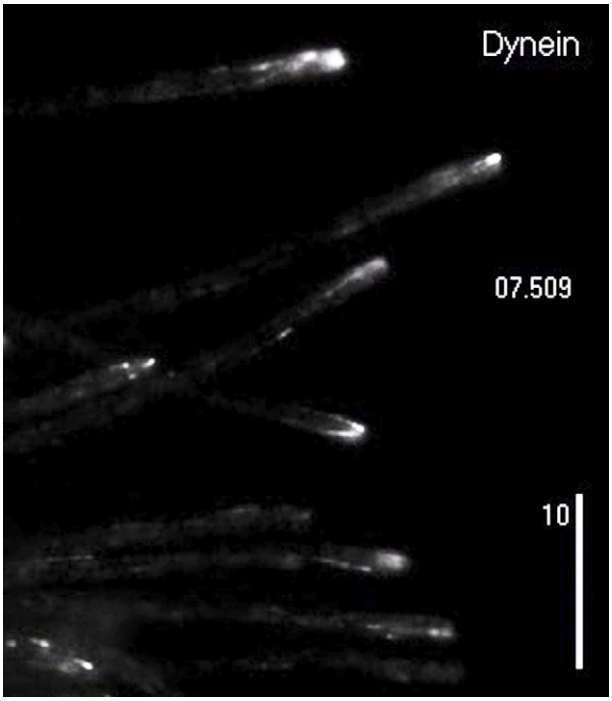

Movie 20 Dynamics of dynein in hyphal cells. Dynein moves bi-directionally and concentrates at the microtubule plus-ends near the hyphal tip. Note that anterograde motility of dynein in fungi is most likely due to the activity of kinesin-1 (Zhang *et al.*, 2003; Lenz *et al.* 2006). Dynein

Author's personal copy

motors were labelled by fusing a triple GFP tag to the N-terminus of the *dyn2* dynein heavy chain gene. The construct is integrated in the native locus; therefore native levels of the motors are shown. The time is given in seconds: milliseconds; the bar represents 10 μm. Click here or on image to access the movie.

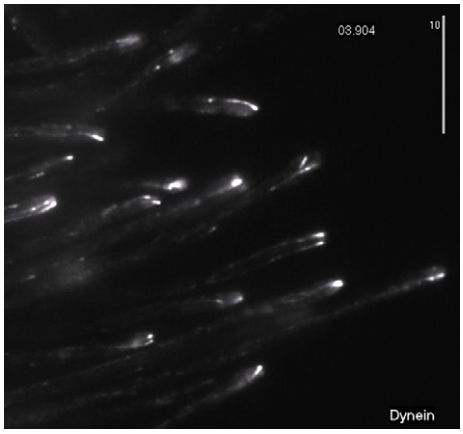

Movie 21 Dynamics of dynein in hyphal cells. A second example of dynein motility in hyphae. Note that the cell usually contains 2 tracks for bi-directional motility of the motor. Dynein motors were labelled by fusing a triple GFP tag to the N-terminus of the *dyn2* dynein heavy chain gene. The construct is integrated in the native locus; therefore native levels of the motors are shown. The time is given in seconds: milliseconds; the bar represents 20 μm. Click here or on image to access the movie.

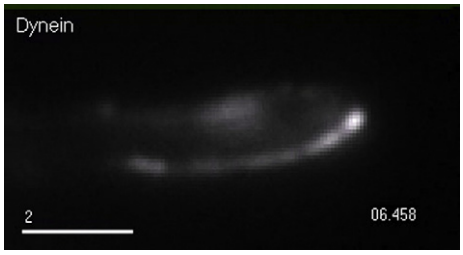

Movie 22 Dynamics of dynein at a microtubule plus-end near the hyphal tip. Dynein forms a "comet-like" accumulation at the end of microtubules that captures arriving endosomes for retrograde motility so that they do not fall off the track (Schuster *et al.*, 2011(a)). Dynein motors were labelled by fusing a triple GFP tag to the N-terminus of the *dyn2* dynein heavy chain gene. The construct is integrated in the native locus, therefore native levels of the motors are shown. The time is given in seconds: milliseconds; the bar represents 2 μm. Click here or on image to access the movie.

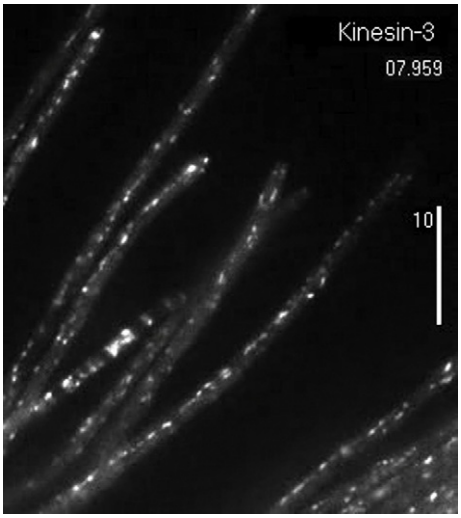

Movie 23 Dynamics of kinesin-3 in hyphal cells. Kinesin-3-GFP continuously move in a bi-directional fashion. Note that the microtubule plus-ends are concentrated at the hyphal tip (Lenz *et al.*, 2006; Schuchardt *et al.*, 2005) and that transport towards the hyphal tips is driven by kinesin-3. In contrast, retrograde transport back to the cell centre is mediated by dynein (Schuster *et al.*, 2011(a)). Kinesin-3 was labelled by fusing eGFP to its C-terminal. The construct is integrated in the native locus; therefore native levels of the motors are shown. The time is given in seconds: milliseconds; the bar represents 10 μm. Click here or on image to access the movie.

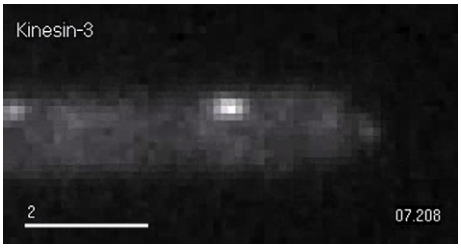

Movie 24 Dynamics of kinesin-3 at the hyphal tip. Kinesin-3-GFP signals travel towards the plus-ends at the hyphal tip, where they turn around for retrograde motility towards the cell centre. Note that retrograde motility is driven by dynein (Schuster *et al.*, 2011(a)). Kinesin-3 was labelled by fusing GFP to its C-terminal. The construct is integrated in the native locus; therefore native levels of the motors are shown. The time is given in seconds: milliseconds; the bar represents 2 μm.Click here or on image to access the movie.

Early endosomes

Movie 25 Early endosomes distribution in a hyphal cell. The organelles are evenly scattered along the length of the

Author's personal copy

hypha. The 3D reconstruction was built from of a deconvolved Z-axis image stack taken after fixing the cells with 0.1 % formaldehyde. Motility of early endosomes was inhibited by a 5 min pre-treatment with 0.1 % formaldehyde. Early endosomes were labelled by a fusion of eGFP to the small GTPase Rab5a. The bar represents 3 μm. Click here or on image to access the movie.

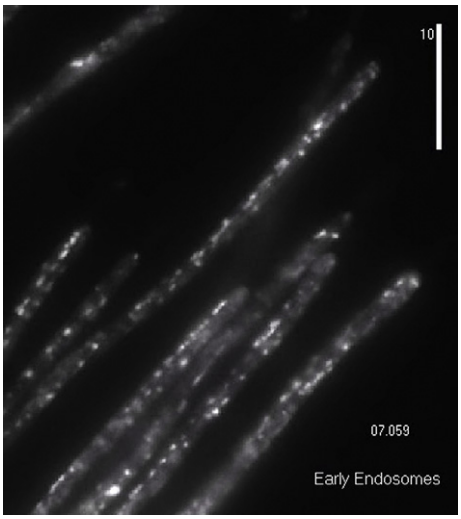

Movie 26 Dynamics of early endosomes in hyphal cells. The organelles move rapidly in a bi-directional fashion. Note that their motility is reminiscent of that of kinesin-3 (Movie 23). Early endosomes were labelled by a fusion of eGFP to the small GTPase Rab5a. The time is given in seconds: milliseconds; the bar represents 10 μm. Click here or on image to access the movie.

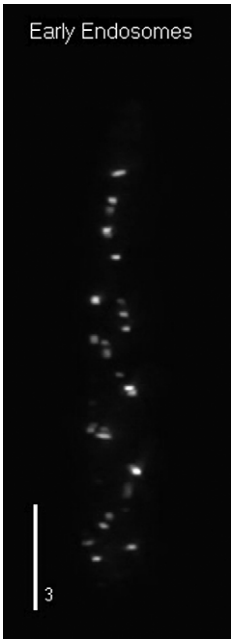

Movie 27 Early endosomes distribution in a yeast-like cell. The organelles are evenly scattered within the budding cell. Motility of early endosomes was inhibited by a 5 minute pre-treatment with 0.1 % formaldehyde.The 3D reconstruction was built from of a deconvolved Z-axis image stack taken after fixing the cells with 0.1 % formaldehyde. Early endosomes were labelled by a fusion of eGFP to the small GTPase Rab5a. The bar represents 3 μm. Click here or on image to access the movie.

Movie 28 Dynamics of early endosomes in a yeast-like cell. The organelles move rapidly in a bi-directional fashion. Note that their motility path is reminiscent of the microtubule organisation (see Movie 4, Movie 5). Early endosomes were labelled by a fusion of eGFP to the small GTPase Rab5a. The time is given in seconds: milliseconds; the bar represents 5 μm. Click here or on image to access the movie.

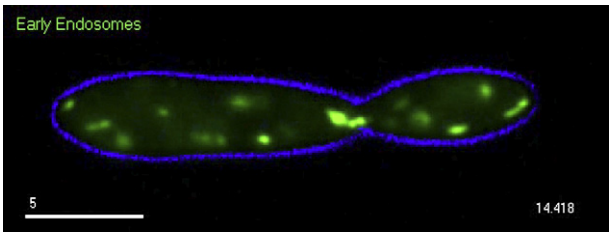

Movie 29 Dynamics of early endosomes in yeast-like cell. The organelles move rapidly in a bi-directional fashion. Note that their motility path is reminiscent of the microtubule organisation (see Movie 4, Movie 5). The cell edge is given in blue, the early endosomes are shown in green. Early endosomes were labelled by a fusion of eGFP to the small GTPase Rab5a. The time is given in seconds: milliseconds; the bar represents 5 μm. Click here or on image to access the movie.

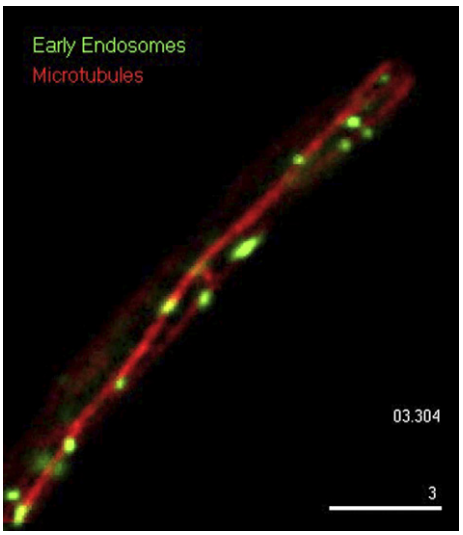

Movie 30 Motility of early endosomes along microtubules in a hyphal cell. The organelles move rapidly in a bi-directional fashion along single microtubules or microtubule

Author's personal copy

bundles (indicated by their brighter fluorescence). Note that the organelles do not fall off the end of the microtubules, but rather rapidly turn for retrograde motility, which is due to loading onto dynein that concentrates at the ends of the microtubules (see Movie 22). The cell edge is given in blue, the early endosomes are shown in green. Early endosomes were labelled by a fusion of eGFP to the small GTPase Rab5a. Microtubules were visualised by monomeric red fluorescent protein (mRFP) fused to the alpha-tubulin gene *tub1*. The time is given in seconds: milliseconds; the bar represents 3 μm. Click here or on image to access the movie.

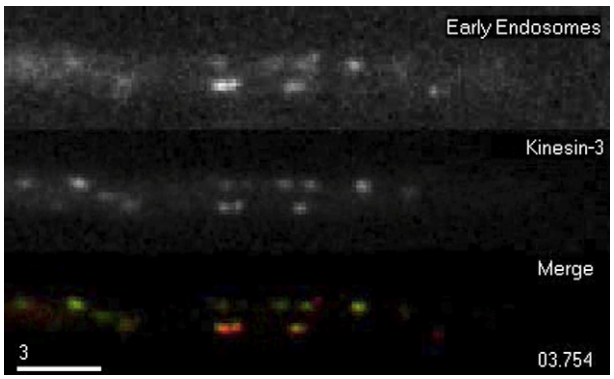

Movie 31 Co-localisation of early endosomes and kinesin-3 in a hyphal cell. All organelles carry kinesin-3, which takes the early endosomes towards the hyphal tip and into the pre-bleached region of the hypha (red box, "bleach"). Pre-bleaching was done to reduce the signal interference. Note that some organelles turn for retrograde motility before reaching the end of the microtubules (arrowhead). Early endosomes were labelled by a fusion of monomeric Cherry to the small GTPase Rab5a. Kinesin-3 was labelled by fusing eGFP to its C-terminal. The construct is ectopically expressed under the kinesin-3 promoter in a deletion background, therefore native levels of the motors are shown. The time is given in seconds: milliseconds; the bar represents 3 μm. Click here or on image to access the movie.

Vacuoles

Movie 32 Vacuole distribution in a hyphal cell. The irregular organelles are evenly scattered along the length of the hypha. Note that the organisation of the vacuolar compartment in hyphae differs significantly from that in yeast-like cells (Movie 34). Vacuoles are labelled by carboxypeptidase Y fused to a triple red fluorescent protein. The 3D reconstruction was built from a deconvolved Z-axis image stack. The bar represents 5 μm. Click here or on image to access the movie.

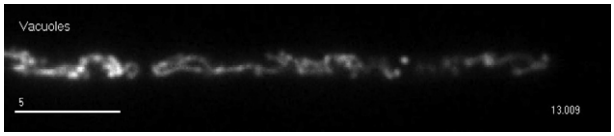

Movie 33 Dynamics of vacuoles in a hyphal cell. The organelles remain almost stationary during the course of observation. Vacuoles are labelled by carboxypeptidase Y fused to a triple red fluorescent protein. The time is given in seconds: milliseconds; the bar represents 5 μm. Click here or on image to access the movie.

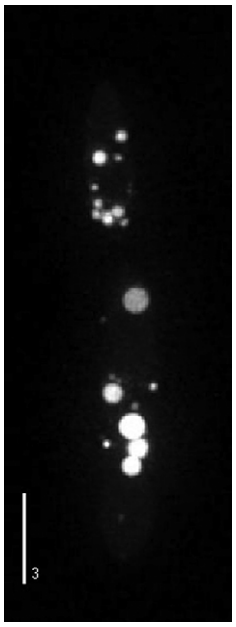

Movie 34 Vacuole distribution in a yeast-like cell. The organelles are spherical and evenly scattered throughout the cell. Note that the number and size of the vacuoles can vary and depends on unknown environmental conditions. Vacuoles were labelled by the dye Cell Tracker Blue (Molecular Probes). The 3D reconstruction was built from a deconvolved Z-axis image stack. The bar represents 3 μm. Click here or on image to access the movie.

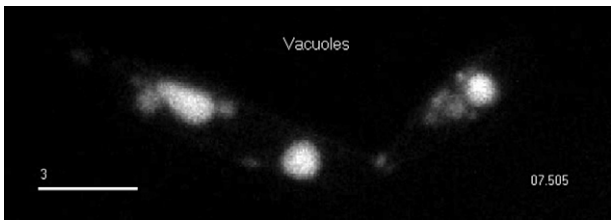

Movie 35 Dynamics of vacuoles in a yeast-like cell. Most of the spherical organelles remain almost stationary during the course of observation. However, small vacuoles show directed movement. In addition, large vacuoles undergo changes in shape (arrowhead). Vacuoles are labelled by carboxypeptidase Y fused to a triple red fluorescent protein. The time is given in seconds: milliseconds; the bar represents 3 μm. Click here or on image to access the movie.

Author's personal copy

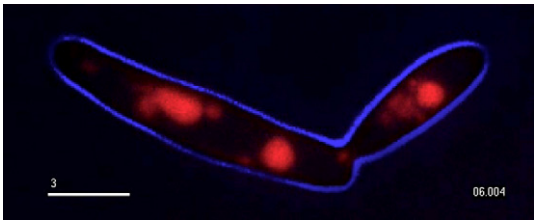

Movie 36 Dynamics of vacuoles in a yeast-like cell. Most of the spherical organelles remain almost stationary during the course of observation. However, small vacuoles show directed movement. In addition, large vacuoles undergo changes in shape (arrowhead). The cell edge is given in blue, the vacuoles are shown in red. Vacuoles are labelled by carboxypeptidase Y fused to a triple red fluorescent protein. The time is given in seconds: milliseconds; the bar represents 3 μm. Click here or on image to access the movie.

Plasma membrane

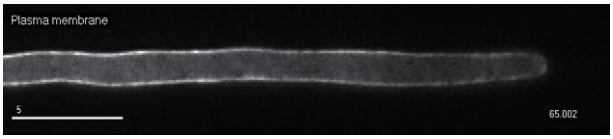

Movie 37 Dynamics of the plasma membrane in a hyphal cell. The plasma membrane was labelled by a fusion protein of eGFP and a Sso1-like syntaxin. The time is given in seconds: milliseconds; the bar represents 5 μm. Click here or on image to access the movie.

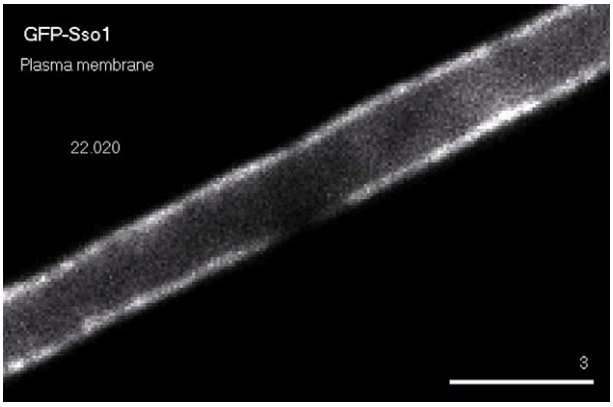

Movie 38 Fluorescent recovery after photo-bleaching (FRAP) experiment in the sub-apical region of the plasma membrane in a hyphal cell. The fluorescence was bleached by a 405 nm laser pulse (red circle, bleach). With time the un-bleached molecules from neighbouring regions of the plasma membrane diffuse into the darkened area. This indicates that molecules can "swim" within the bi-layer. This experiment nicely illustrates the "fluid mosaic model" that was suggested decades ago (Singer and Nicolson, 1972). The plasma membrane was labelled by a fusion protein of eGFP and a Sso1-like syntaxin. The time is given in seconds: milliseconds; the bar represents 5 μm. Click here or on image to access the movie.

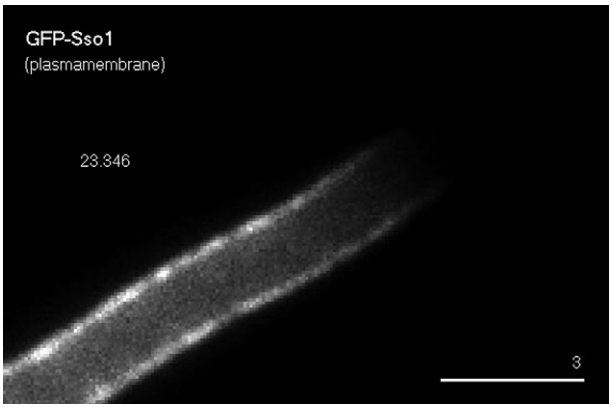

Movie 39 Fluorescent recovery after photo-bleaching (FRAP) experiment in the apical region of the plasma membrane in a hyphal cell. The fluorescence was bleached by a 405 nm laser pulse (red circle, bleach). The un-bleached molecules from neighbouring regions of the plasma membrane do not diffuse into the darkened area. This indicates that the fluidity of the membrane is impaired at the hyphal tip, which is most likely due to an enrichment of sphingolipids (Canovas and Perez-Martin, 2009). The plasma membrane was labelled by a fusion protein of eGFP and a Sso1-like syntaxin. The time is given in seconds: milliseconds; the bar represents 3 μm. Click here or on image to access the movie.

Endoplasmic reticulum

Movie 40 Distribution of the endoplasmic reticulum in a hyphal cell. The irregular network is mainly concentrated at the cell periphery. Note that yeast-like cell contain a more regular network (Movie 43–47). The endoplasmic reticulum and the nuclear envelope was visualised by expressing eGFP, N-terminally fused to a calreticulin signal peptide and C-terminally fused to the retention signal HDEL (Wedlich-Söldner *et al.*, 2002b). The 3D reconstruction was built from a deconvolved Z-axis image stack. The bar represents 5 μm. Click here or on image to access the movie.

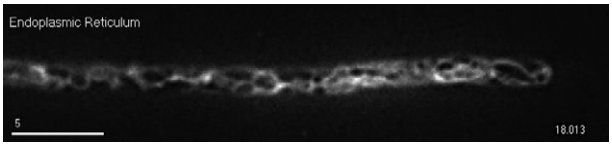

Movie 41 Dynamics of the endoplasmic reticulum in a hyphal cell. The network remains mainly stationary. Occasionally long-range motility occurs (one event

Author's personal copy

indicated by arrowhead). The endoplasmic reticulum and the nuclear envelope was visualised by expressing eGFP, N-terminally fused to a calreticulin signal peptide and C-terminally fused to the retention signal HDEL (Wedlich-Söldner *et al.*, 2002b). The time is given in seconds: milliseconds; the bar represents 5 μm. Click here or on image to access the movie.

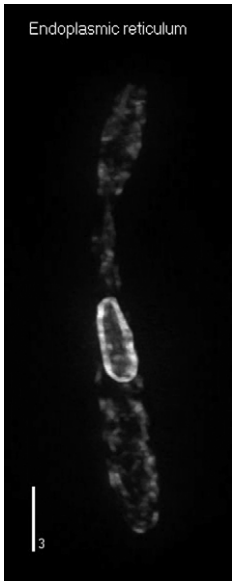

Movie 42 Distribution of the endoplasmic reticulum in a yeast-like cell. The irregular network is mainly concentrated at the cell periphery. The nuclear envelope (spherical structure in the centre of the mother cell) is in contact with the peripheral network. Note that image processing for the 3D reconstruction did not well preserve the character of the network (compare Movie 43–46). The endoplasmic reticulum and the nuclear envelope was visualised by expressing eGFP, N-terminally fused to a calreticulin signal peptide and C-terminally fused to the retention signal HDEL (Wedlich-Söldner *et al.*, 2002b). The 3D reconstruction was built from a deconvolved Z-axis image stack. The bar represents 3 μm. Click here or on image to access the movie.

Movie 43 Dynamics of the endoplasmic reticulum in a yeast-like cell. The peripheral network is undergoing thermal flickering. In addition, directed motility of tubules occurs (arrowhead). Note that this motility is driven by microtubule motors (Wedlich-Söldner *et al.*, 2002b). The bright signal in the cell centre represents the nuclear envelope. The endoplasmic reticulum and the nuclear envelope were visualised by expressing eGFP, N-terminally fused to a calreticulin signal peptide and C-terminally fused to the retention signal HDEL. The time is given in seconds: milliseconds; the bar represents 3 μm. Click here or on image to access the movie.

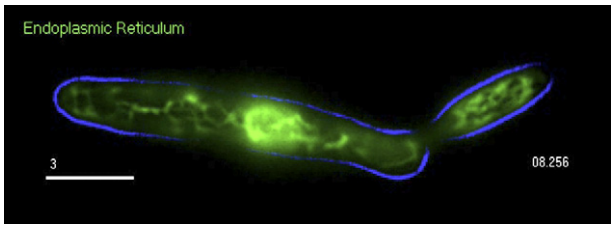

Movie 44 Dynamics of the endoplasmic reticulum in a yeast-like cell. The peripheral network is undergoing thermal flickering. In addition, directed motility of tubules occurs (arrowhead) that is mediated by microtubule motors (Wedlich-Söldner *et al.*, 2002b). The bright signal in the cell centre represents the nuclear envelope. The cell edge is depicted in blue, the endoplasmic reticulum is shown in green. The endoplasmic reticulum and the nuclear envelope was visualised by expressing eGFP, N-terminally fused to a calreticulin signal peptide and C-terminally fused to the retention signal HDEL (Wedlich-Söldner *et al.*, 2002b). The time is given in seconds: milliseconds; the bar represents 3 μm. Click here or on image to access the movie.

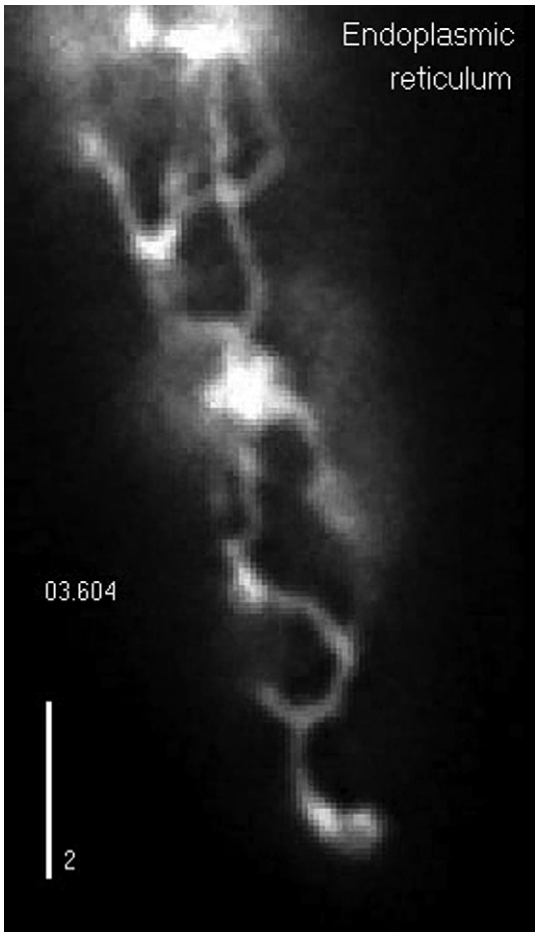

Movie 45 Directed motility of tubules within the endoplasmic reticulum in a yeast-like cell. Bi-directional motility is modulating the peripheral network. The endoplasmic reticulum and the nuclear envelope was visualised by expressing eGFP, N-terminally fused to a calreticulin signal peptide and C-

Author's personal copy

terminally fused to the retention signal HDEL (Wedlich-Söldner *et al.*, 2002b). The time is given in seconds: milliseconds; the bar represents 2 μm. Click here or on image to access the movie.

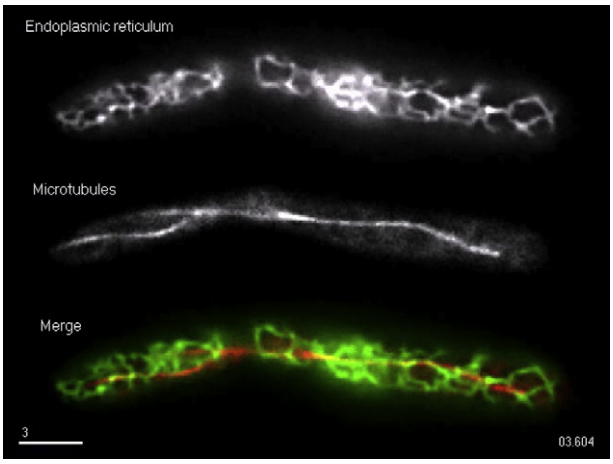

Movie 46 Motility of the endoplasmic reticulum and microtubules. Bi-directional motility occurs around the microtubule tracks. The endoplasmic reticulum and the nuclear envelope was visualised by expressing eGFP, N-terminally fused to a calreticulin signal peptide and C-terminally fused to the retention signal HDEL (Wedlich-Söldner *et al.*, 2002b). The microtubules were visualised by monomeric Cherry fused to the alpha-tubulin gene *tub1*. The time is given in seconds: milliseconds; the bar represents 3 μm. Click here or on image to access the movie.

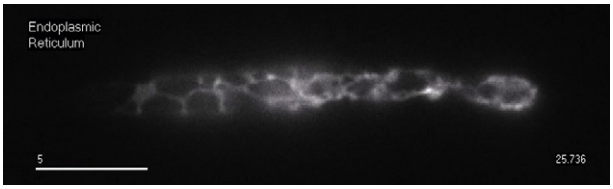

Movie 47 Fluorescent recovery after photo-bleaching (FRAP) experiment showing diffusion within the endoplasmic reticulum in a yeast-like cell. The fluorescence is bleached by a 405 nm laser pulse (bright signal, moving from left to right). Un-bleached molecules within the network diffuse into the darkened area, showing that the tubules of the endoplasmic reticulum are connected. The endoplasmic reticulum and the nuclear envelope was visualised by expressing eGFP, N-terminally fused to a calreticulin signal peptide and C-terminally fused to the retention signal HDEL (Wedlich-Söldner *et al.*, 2002b). The time is given in seconds: milliseconds; the bar represents 5 μm. Click here or on image to access the movie.

Golgi apparatus

Movie 48 Distribution of the Golgi apparatus in a hyphal cell. The Golgi consists of small vesicles that are found all along the length of the cell, but concentrate at the hyphal tip. The Golgi vesicles were visualised by a fusion of the small GTPase Ypt1 and eGFP (Wedlich-Söldner *et al.*, 2002b). 3D reconstruction was built from a Z-axis image stack. The bar represents 5 μm. Click here or on image to access the movie.

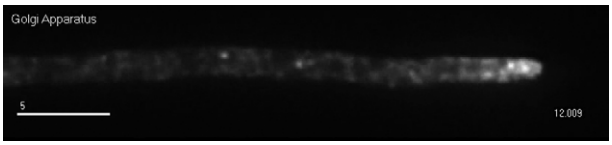

Movie 49 Dynamics of Golgi vesicles in a hyphal cell. The Golgi membranes seem to be in constant motion. It is not clear from this movie whether this is due to rapid bi-directional motility or Brownian motion. The Golgi vesicles were visualised by a fusion of the small GTPase Ypt1 and eGFP (Wedlich-Söldner *et al.*, 2002b). The time is given in seconds: milliseconds; the bar represents 5 μm. Click here or on image to access the movie.

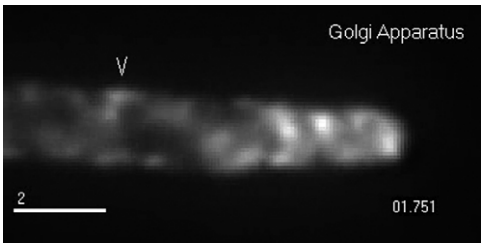

Movie 50 Directed motility of Golgi membranes near the hyphal tip. A Golgi vesicle rapidly moves towards the hyphal apex. The Golgi vesicles were visualised by a fusion of the small GTPase Ypt1 and eGFP (Wedlich-Söldner *et al.*, 2002b). The time is given in seconds: milliseconds; the bar represents 2 μm. Click here or on image to access the movie.

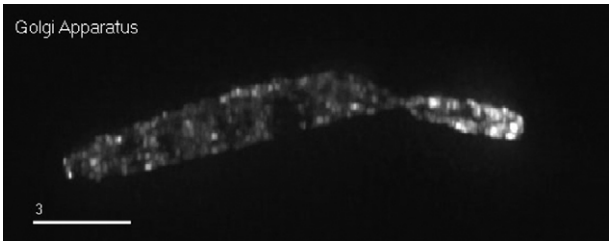

Movie 51 Distribution of the Golgi apparatus in a yeast-like cell. The Golgi consists of small vesicles that are found distributed within the whole cell, but concentrate in the growing bud. The Golgi vesicles were visualised by a fusion of the small GTPase Ypt1 and eGFP (Wedlich-Söldner *et al.*, 2002b). The 3D reconstruction was built from a deconvolved Z-axis image stack. The bar represents 3 μm. Click here or on image to access the movie.

Author's personal copy

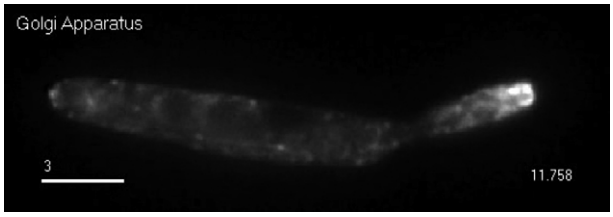

Movie 52 Dynamics of Golgi vesicles in a yeast-like cell. The Golgi membranes seem to be in constant motion. It is not clear from this movie whether this is due to rapid bi-directional motility or Brownian motion. The Golgi vesicles were visualised by a fusion of the small GTPase Ypt1 and eGFP (Wedlich-Söldner *et al.*, 2002b). The time is given in seconds: milliseconds; the bar represents 3 μm. Click here or on image to access the movie.

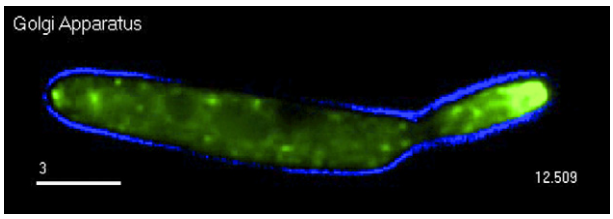

Movie 53 Dynamics of Golgi vesicles in a yeast-like cell. The Golgi membranes seem to be in constant motion. It is not clear from this movie whether this is due to rapid bi-directional motility or Brownian motion. The Golgi vesicles were visualised by a fusion of the small GTPase Ypt1 and eGFP. The time is given in seconds: milliseconds; the bar represents 3 μm. Click here or on image to access the movie.

Chitosomes (chitin synthase 8)

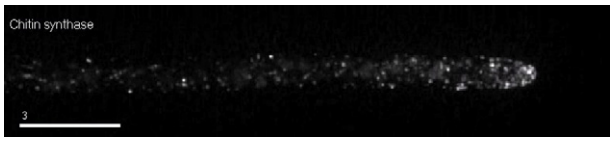

Movie 54 Distribution of Chitin synthase 8 in a hyphal cell. The majority of the membrane-bound chitin synthase is located in the plasma membrane. In addition signals are found in the cytoplasm that most likely represent chitosomes. Note that *U. maydis* contains 7 additional chitin synthases (Weber *et al.*, 2006) that might locate to additional vesicles. Signals represent the membrane-bound chitin synthase 8 fused to a triple GFP tag (Treitschke *et al.*, 2010). The 3D reconstruction was built from a deconvolved Z-axis image stack. The bar represents 3 μm. Click here or on image to access the movie.

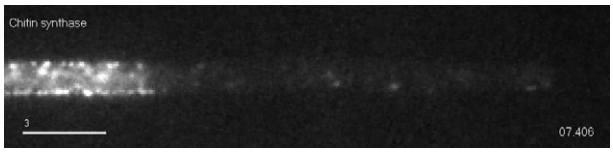

Movie 55 Dynamics of chitin synthase 8-bound chitosomes in a hyphal cell. Whereas the plasma membrane-bound chitin synthase is fairly stationary, the vesicle-bound fraction moves within the cell. This motility is best visible after pre-bleaching areas of the cell with a 405 nm laser. Single signals are moving into the darkened cell region. Note that chitin synthase 8 molecules have a myosin motor domain and are therefore also considered to belong to the class XVII myosins. However, the observed motility depends on microtubules but also requires F-actin (Treitschke *et al.*, 2010). Signals represent the membrane-bound chitin synthase 8 fused to a triple GFP tag (Treitschke *et al.*, 2010). The time is given in seconds: milliseconds; the bar represents 3 μm. Click here or on image to access the movie.

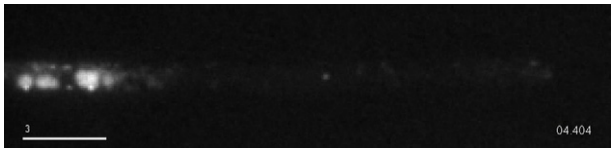

Movie 56 Dynamics of chitosomes, labelled with chitin synthase lacking the myosin motor domain, in a hyphal cell. The vesicle-bound fraction of the truncated chitin synthase still moves within the cell. This motility is best visible after pre-bleaching areas of the cell with a 405 nm laser. Thus the motor domain of chitin synthase is not required for long-range motility (Treitschke *et al.*, 2010). Signals represent a truncated version of the membrane-bound chitin synthase 8, missing the motor domain, fused to a triple GFP tag (Treitschke *et al.*, 2010). The time is given in seconds: milliseconds; the bar represents 3 μm. Click here or on image to access the movie.

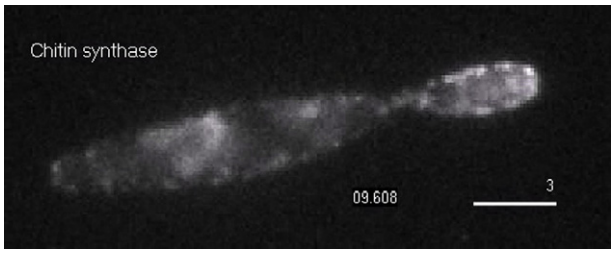

Movie 57 Dynamics of chitin synthase 8-bound chitosomes in a yeast-like cell. The plasma membrane-bound chitin synthase concentrates at the growing bud. Occasionally, chitosomes are seen that rapidly move within the cell. Signals represent the membrane-bound chitin synthase 8 fused to a triple GFP tag (Treitschke *et al.*, 2010). The time is given in seconds: milliseconds; the bar represents 3 μm. Click here or on image to access the movie.

Author's personal copy

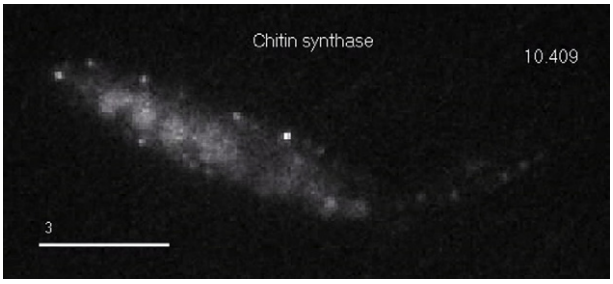

Movie 58 Dynamics of chitin synthase 8-bound chitosomes in a yeast-like cell. After pre-bleaching the bud with a 405 nm laser (red box, "Bleach"), motility of GFP-labelled chitin synthase becomes visible. Signals represent the membrane-bound chitin synthase 8 fused to a triple GFP tag (Treitschke *et al.*, 2010). The time is given in seconds: milliseconds; the bar represents 3 μm. Click here or on image to access the movie.

Nucleus

Movie 59 Dynamics of the nucleus in a hyphal cell. The elongated nucleus is stationary, but motors exert forces onto the nuclear envelope and pull extensions out of the organelle. In yeast-like cells this motility is due to dynein (Straube *et al.*, 2001, 2005). The nucleus was labelled by a triple RFP tag fused to a nuclear localisation signal (Straube *et al.*, 2005). The time is given in seconds: milliseconds; the bar represents 5 μm. Click here or on image to access the movie.

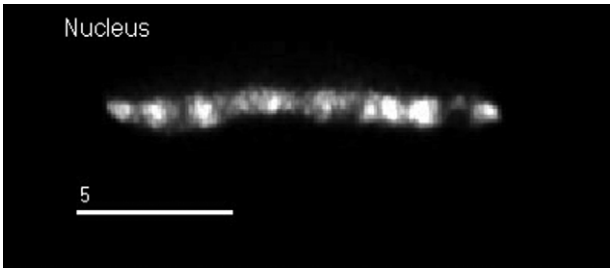

Movie 60 Shape of an elongated nucleus in a hyphal cell. The 3D reconstruction was built from of a deconvolved Z-axis image stack. The nucleus was labelled by a triple RFP tag fused to a nuclear localisation signal (Straube *et al.*, 2005). The bar represents 5 μm.Click here or on image to access the movie.

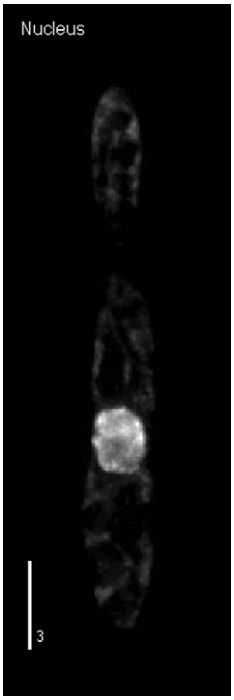

Movie 61 The nucleus in a yeast-like cell. The nucleus was labelled by a triple RFP tag fused to a nuclear localisation signal (Straube *et al.*, 2005). The 3D reconstruction was built from a deconvolved Z-axis image stack. The bar represents 3 μm. Click here or on image to access the movie.

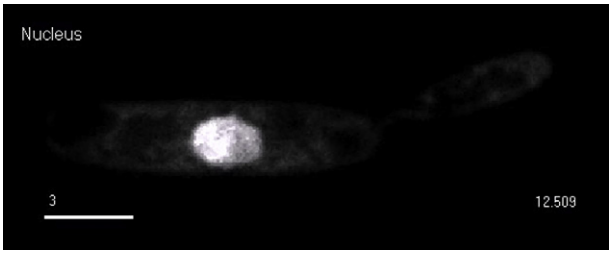

Movie 62 Dynamics of the nucleus in a yeast-like cell. The nucleus is stationary, but motors exert forces onto the nuclear envelope and pull extensions out of the organelle. This motility is mediated by dynein (Straube *et al.*, 2001, 2005). The nucleus was labelled by a triple RFP tag fused to a nuclear localisation signal (Straube *et al.*, 2005). The time is given in seconds: milliseconds; the bar represents 5 μm. Click here or on image to access the movie.

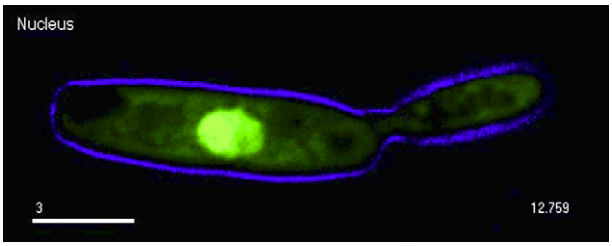

Movie 63 Dynamics of the nucleus in a yeast-like cell. The nucleus is stationary, but motors exert forces onto the

Author's personal copy

nuclear envelope and pull extensions out of the organelle. This motility is mediated by dynein (Straube *et al.*, 2001, 2005). The nucleus was labelled by a triple RFP tag fused to a nuclear localisation signal (Straube *et al.*, 2005). The cell edge is shown in blue, the nucleus in green. The time is given in seconds: milliseconds; the bar represents 3 μm. Click here or on image to access the movie.

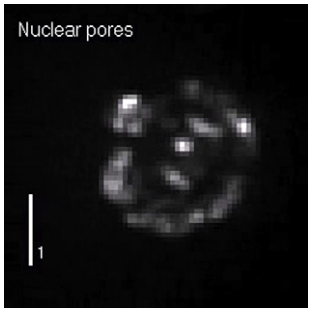

Movie 64 Nuclear pores in a yeast-like cell. The pores were labelled by a fusion of the nuclear porin Nup107 and eGFP (Theisen *et al.*, 2008). The 3D reconstruction was built from a deconvolved Z-axis image stack. The bar represents 1 μm. Click here or on image to access the movie.

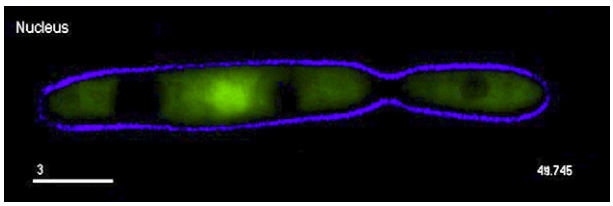

Movie 65 Fluorescent recovery after photo-bleaching (FRAP) experiment showing nuclear import into a nucleus in a yeast-like cell. The fluorescence in the nucleus is bleached by a 405 nm laser pulse (red box, "Bleach" in second frame). The fluorescent signal inside the nucleus slowly recovers due to the import of un-bleached GFP-reporter proteins from the cytoplasm. The nucleus was labelled by a triple RFP tag fused to a nuclear localisation signal (Straube *et al.*, 2005). The time is given in seconds: milliseconds; the bar represents 3 μm. Click here or on image to access the movie.

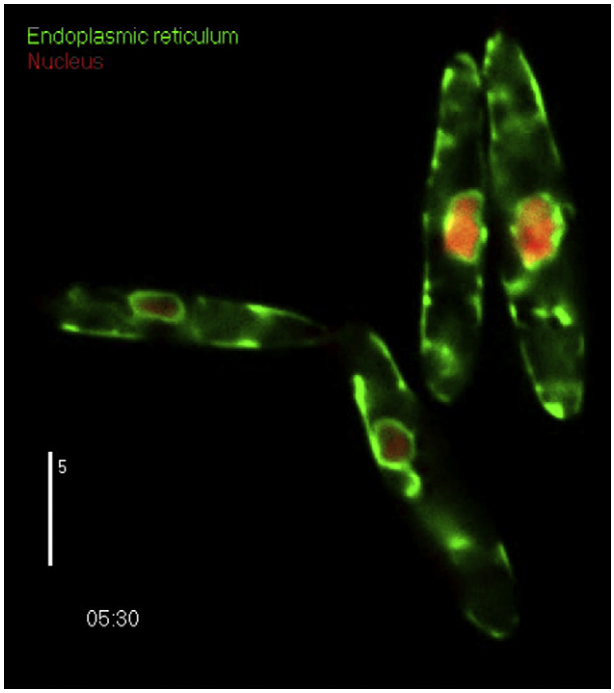

Movie 66 Nuclear import in a post-mitotic cell. The endoplasmic reticulum (green) forms new nuclear envelopes in telophase (arrowheads). The chromosomes de-condense and the nuclei grow in size. At this stage the nuclear pores reassemble (Theisen *et al.*, 2008) and import of nuclear proteins start. Note that two additional interphase cells are shown. The nucleus was labelled by a triple RFP tag fused to a nuclear localisation signal (Straube *et al.*, 2005). The endoplasmic reticulum and the nuclear envelope was visualised by expressing eGFP, N-terminally fused to a calreticulin signal peptide and C-terminally fused to the retention signal HDEL. The time is given in seconds: milliseconds; the bar represents 5 μm. Click here or on image to access the movie.

Peroxisomes

Movie 67 Distribution of peroxisomes in a hyphal cell. The peroxisomes are evenly distributed. Peroxisomes were labelled by eGFP fused to the import tri-peptide SKL. The 3D reconstruction was built from a deconvolved Z-axis image stack. The bar represents 5 μm. Click here or on image to access the movie.

Movie 68 Dynamics of peroxisomes in a hyphal cell. Most peroxisomes are stationary or undergo Brownian motion.

Author's personal copy

Occasionally, peroxisomes show rapid bi-directional motility. Note that the halos result from peroxisomes that are not in focus. Peroxisomes were labelled by eGFP fused to the import tri-peptide SKL. The time is given in seconds: milliseconds; the bar represents 5 μm. Click here or on image to access the movie.

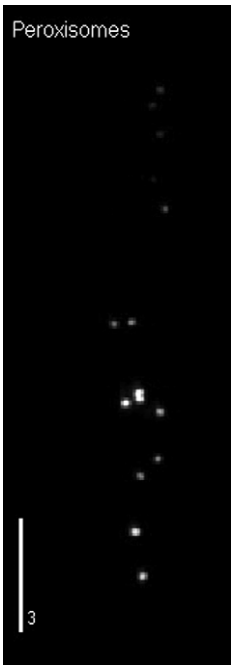

Movie 69 Distribution of peroxisomes in a yeast-like cell. The peroxisomes are evenly distributed. Peroxisomes were labelled by eGFP fused to the import tri-peptide SKL. The 3D reconstruction was built from a deconvolved Z-axis image stack. The bar represents 3 μm. Click here or on image to access the movie.

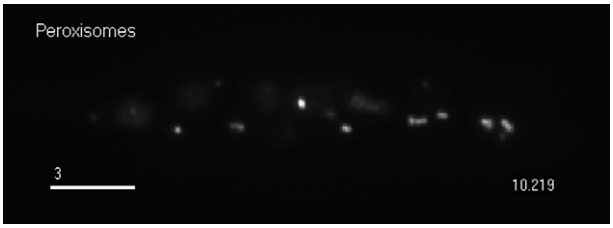

Movie 70 Dynamics of peroxisomes in a yeast-like cell. Most peroxisomes are stationary or undergo Brownian motion. Occasionally, peroxisomes show rapid bi-directional motility. Note that the halos result from peroxisomes that are not in focus. Peroxisomes were labelled by eGFP fused to the import tri-peptide SKL. The time is given in seconds: milliseconds; the bar represents 3 μm. Click here or on image to access the movie.

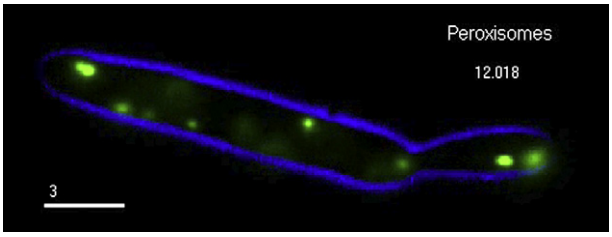

Movie 71 Dynamics of peroxisomes in a yeast-like cell. Most peroxisomes are stationary or undergo Brownian motion. Occasionally, peroxisomes show rapid bi-directional motility. Note that the halos result from peroxisomes that are not in focus. The cell edge is shown in blue, peroxisomes are shown in green. Peroxisomes were labelled by eGFP fused to the import tri-peptide SKL. The time is given in seconds: milliseconds; the bar represents 3 μm. Click here or on image to access the movie.

Mitochondria

Movie 72 Distribution of mitochondria in a hyphal cell. The elongated organelles are evenly distributed. Mitochondria were labelled by the *U. maydis*-specific matrix protein LGA fused to eGFP (Mahlert *et al.*, 2009). The 3D reconstruction was built from a deconvolved Z-axis image stack. The bar represents 5 μm. Click here or on image to access the movie.

Movie 73 Dynamics of mitochondria in a hyphal cell. Most organelles are stationary or undergo Brownian motion. Occasionally, mitochondria show short range motility (arrowhead). Mitochondria were labelled by the *U. maydis*-specific matrix protein LGA fused to eGFP (Mahlert *et al.*, 2009). The time is given in seconds: milliseconds; the bar represents 5 μm. Click here or on image to access the movie.

Author's personal copy

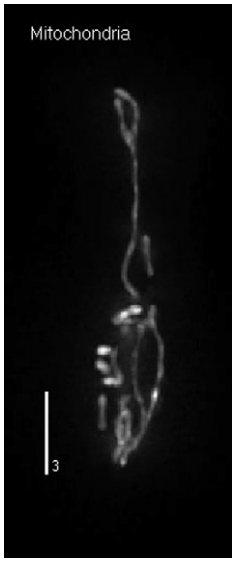

Movie 74 Distribution of mitochondria in a yeast-like cell. The organelles are evenly distributed. Sometimes very long mitochondria are formed. Mitochondria were labelled by the *U. maydis*-specific matrix protein LGA fused to eGFP (Mahlert *et al.*, 2009). The 3D reconstruction was built from a deconvolved Z-axis image stack. The bar represents 3 μm. Click here or on image to access the movie.

Movie 75 Dynamics of mitochondria in a yeast-like cell. The organelles are mainly stationary. Mitochondria were labelled by the *U. maydis*-specific matrix protein LGA fused to eGFP (Mahlert *et al.*, 2009). The time is given in seconds: milliseconds; the bar represents 3 μm. Click here or on image to access the movie.

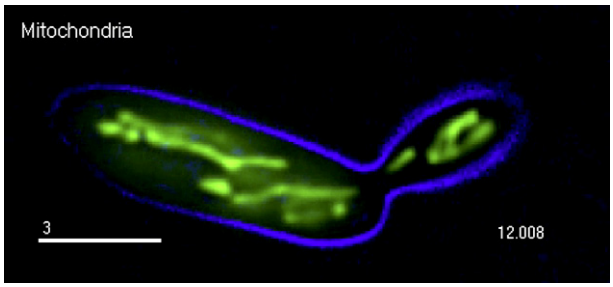

Movie 76 Dynamics of mitochondria in a yeast-like cell. The organelles are mainly stationary. The cell edge is shown in blue, peroxisomes are shown in green. Mitochondria were labelled by the *U. maydis*-specific matrix protein LGA fused to eGFP (Mahlert *et al.*, 2009). The time is given in seconds: milliseconds; the bar represents 3 μm. Click here or on image to access the movie.

Concluding remarks

In this article we provide a comprehensive collection of movies that illustrate the distribution (Fig. 3) and dynamic behaviour of organelles, motors and the filaments of the cytoskeleton in a living fungal cell. The provided imaging data reveal two noticeable features. Firstly, most organelles are evenly scattered and they seem to perform their cellular function along the whole length of the hyphal cell. A filamentous fungal cell grows at the hyphal tip and forms septa at the rear cell pole. It seems obvious that communication between both ends is necessary. Active transport of early endosomes along the cytoskeleton and diffusion within continuous membranous compartments, such as the endoplasmic reticulum or the vacuoles might support long-range communication or material transport (Steinberg, 2007b; Darrah *et al.*, 2006; Fricker *et al.*, 2008; Zhuang *et al.*, 2009). However, we are far from understanding the communication routes in hyphal cells. Secondly, organelles show very different dynamic behaviour, with early endosomes continuously moving, whereas mitochondria and peroxisomes are mainly immobile. Interestingly, even these more stationary organelles have the capacity to travel along the cytoskeleton. This point is best illustrated in Movie 68 and Movie 73. Whereas major progress has been made in understanding the molecular basis of this motility, the reason for the difference in the dynamic behaviour of organelles is still elusive. An integrative understanding of the fungal cell will require to bridge between the questions "how do organelles move?" and "why do organelles move?".

Methods

Labelling sub-cellular structures and compartments

Microtubules. These fibres of the cytoskeleton were labelled by enhanced green fluorescent protein (eGFP), monomeric red fluorescent protein (mRFP) or monomeric Cherry fused to the N-terminus of the α-tubulin gene *tub1* (Steinberg *et al.*, 2001). The construct is expressed under the constitutive *otef* promoter as an additional copy. Similar fusion proteins were used in other fungi (Ding *et al.*, 1998; Carminati and Stearns, 1997; Han *et al.*, 2001; Su *et al.*, 2004; Horio and Oakley, 2005).

F-Actin. Filamentous actin was stained by fusing eGFP to a modified Lifeact-peptide, representing the first 17 amino acids of the actin-binding protein Abp140 (Riedl *et al.*, 2008). A similar construct was used to visualise actin dynamics in *N. crassa* (Berepiki *et al.*, 2010; Delgado-Alvarez *et al.*, 2010). The construct was expressed under the constitutive *otef* promoter.

Molecular motors. Myosin-5 was labelled by fusing a triple eGFP tag to the N-terminus of the myo5 heavy chain (Weber *et al.*, 2003). Kinesin-3 was visualised by fusing eGFP fused to the C-terminus of *kin3* (Schuchardt *et al.*, 2005). The dynein motor complex was labelled by a fusion of a triple-eGFP and the *dyn2* dynein heavy chain gene (Straube *et al.*, 2001).

Author's personal copy

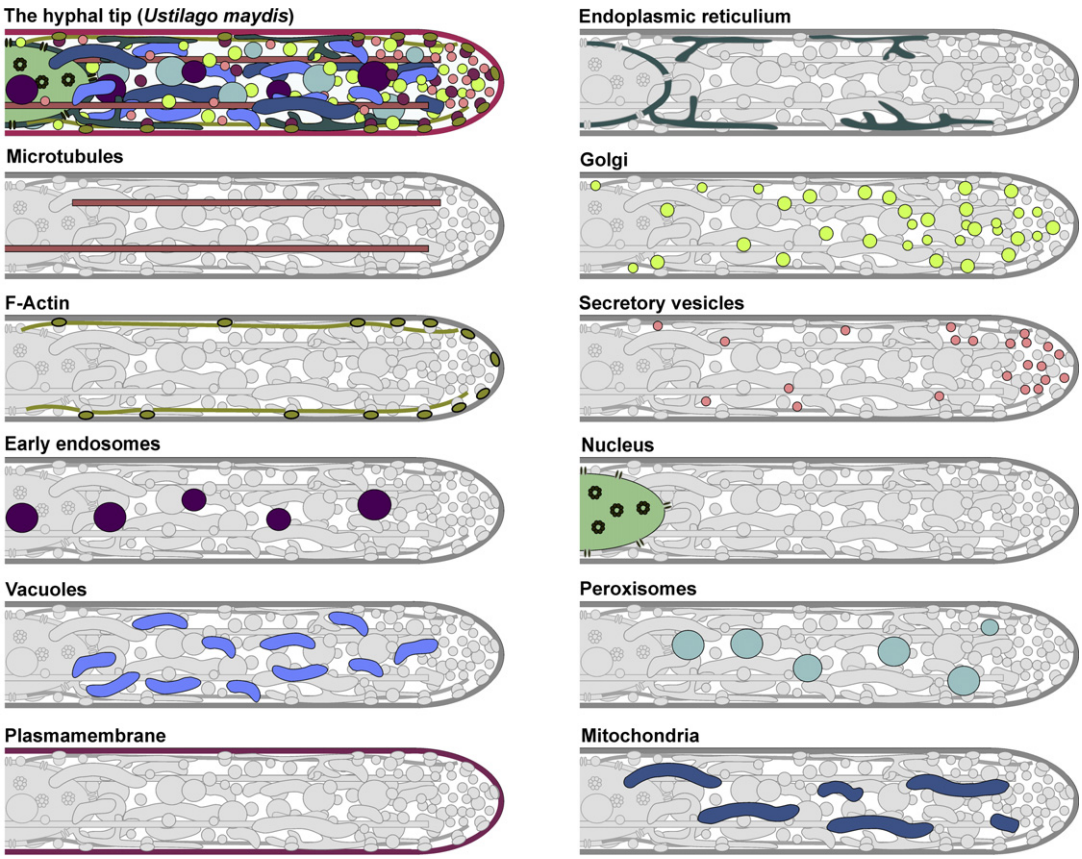

Fig. 3 – The distribution of sub-cellular structures in a hyphal cell. Graphical representation of the organisation of a hyphal cell in *U. maydis*. The Figure summarises the distribution of sub-cellular structures shown in the movies provided alongside with this article.

All constructs were integrated into the native loci. The observed signals therefore represent the native levels of the respective molecular motors. Motors have also been visualised in *A. nidulans* (Han *et al.*, 2001; Konzack *et al.*, 2005; Zekert and Fischer, 2009; Zhang *et al.*, 2010).

Early endosomes. These organelles were visualised using fusions of eGFP or mCherry with the small GTPase Rab5a, which localises on early endosomes (Fuchs *et al.*, 2006). The construct was expressed under the constitutive *otef* promoter. A comparable approach was used for *A. nidulans* (Abenza *et al.*, 2009).

Vacuoles. Carboxypeptidase Y, a well established marker for fungal vacuoles (Klionsky *et al.*, 1990) was visualised by fusing a triple mRFP tag to its C-terminal end. The construct was expressed under the *otef* promoter. A similar construct was used before in *A. oryzae* (Ohneda *et al.*, 2002).

Plasma membrane. The plasma membrane was labelled by eGFP fused to the N-terminus of the *U. maydis* homologue of the syntaxin Sso1p (Aalto *et al.*, 1993). This protein was previously shown to localise in the plasma membrane of *U. maydis* (Treitschke *et al.*, 2010). The fusion protein was expressed under the constitutive *otef* promoter.

Endoplasmic reticulum. The lumen of this compartment was visualised by a construct consisting of the first 17 amino acids of calreticulin from rabbit fused to eGFP, followed by an ER retention signal HDEL (Wedlich-Söldner *et al.*, 2002b).

Golgi. The Golgi apparatus was labelled by a homologue of the Rab GTPase *ypt1* (Segev *et al.*, 1988; Preuss *et al.*, 1992; Kamena *et al.*, 2008). The construct used here consisted of eGFP fused to the N-terminus of the *U. maydis* homologue of Ypt1, expressed under the constitutive *otef* promoter (Wedlich-Söldner *et al.*, 2002b).

Nucleus. Protein import into the nucleus is mediated by localisation signals (Lange *et al.*, 2007). Such NLS were found in various fungal proteins and there location in the nucleus was verified (Vauchelles *et al.*, 2010; Kim *et al.*, 2010) We made use of a construct consisting of a nuclear localisation signal of the GAL-4 DNA binding domain from a commercially available vector, fused to a triple mRFP tag and expressed under the constitutive *otef* promoter (Straube *et al.* 2001; Straube *et al.*, 2005; Theisen *et al.*, 2008).

Nuclear pores. Passage in and out of the nucleus occurs *via* nuclear pores (Capelson and Hetzer, 2009). The pores in *U. maydis* were labelled by a fusion of the nuclear porin gene *nup107* to eGFP (Theisen *et al.*, 2008). The construct was integrated into the native genomic locus.

Peroxisomes. These organelles were labelled by an eGFP–SKL fusion construct, which was expressed under the constitutive *otef* promoter. The SKL tag is recognised by the peroxisomal import machinery and similar constructs were used to visualise fungal peroxisomes (Lewin *et al.*, 1990; Valenciano *et al.*, 1998; Idnurm *et al.*, 2007; Imazaki *et al.*, 2010).

Author's personal copy

Table 1 – Strains and plasmids used in this study.

AB33	*a2 PnarbW2 PnarbE1, ble*^{R}	Brachmann *et al.*, 2001
AB33GT	*a2 PnarbW2 PnarbE1, ble*^{R}/potefGFPTub1	Schuster *et al.*, 2011(b)
AB33GLifeact	*a2 PnarbW2 PnarbE1, ble*^{R}/poGLifeact	Schuster *et al.*, submitted for publication
AB33 G_3Myo5	*a2 PnarbW2 Pnar-bE1, Pmyo5-3xegfp-myo5, ble*^{R}, *hyg*^{R}	Schuster *et al.*, submitted for publication
AB33G_3Dyn2	*a2 PnarbW2 Pnar-bE1, Pdyn2-3xegfp-dyn2, ble*^{R}, *hyg*^{R}	Lenz *et al.*, 2006
AB33Kin3G	*a2 PnarbW2 Pnar-bE1, Pkin3-kin3-egfp, ble*^{R}, *hyg*^{R}	Schuster *et al.*, 2011(b)
AB33GRab5a	*a2 PnarbW2 PnarbE1, ble*^{R}/poGRab5a	Schuster *et al.*, 2011(a)
AB33GRab5a_RTub1	*a2 PnarbW2 PnarbE1, ble*^{R}/poGRab5a/pRFPTub1	Fuchs *et al.*, 2005(b)
AB33ΔKin3_Kin3G_ChRab5a	*a2 PnarbW2 PnarbE1, Δkin3, ble*^{R}, *hyg*^{R}/pkin3G/po$_m$ChRab5a	Schuster *et al.*, 2011(b)
AB33paGRab5a_CpYR	*a2 PnarbW2 PnarbE1, ble*^{R}/popaGRab5a/poCpyR	This study
AB33GSso1	*a2 PnarbW2 PnarbE1, ble*^{R}/poGSso1	This study
AB33EG	*a2 PnarbW2 PnarbE1, ble*^{R}/pERGFP	Wedlich-Söldner *et al.*, 2002(a)
FB1GYPT	*a1b1*/pGFPYpt1	Wedlich-Söldner *et al.*, 2002(a)
AB33 pERGFP_po$_m$ChTub1	*a2 PnarbW2 PnarbE1, ble*^{R}/pERGFP/po$_m$ChTub1	This study
AB33Mcs1G_3	*a2 PnarbW2 Pnar-bE1, Pmcs1-mcs1-3xegfp, ble*^{R}, *hyg*^{R}	Schuster *et al.*, 2011(b)
SG200G_3Mcs1ΔMM	*a1 mfa2 bW2 bE, bl*^{R}*e, Δmcs1::hyg*^{R}/pn3GMcs1ΔMM	Treitschke *et al.*, 2010
AB33nRFP	*a2 PnarbW2 PnarbE1, ble*^{R}/pN_NLS3xRFP	Schuster *et al.*,
FB2N107G_ER	*a2b2 Pnup107-nup107-egfp, ble*^{R}/pERRFP	Theisen *et al.*, 2008
FB2nRFP-ERG	*a2b2*/pC_NLS3xRFP/pN_ERGFP	Straube *et al.*, 2005
AB33GSKL	*a2 PnarbW2 PnarbE1, ble*^{R}/poGSKL	This study
AB33LgaG	*a2 PnarbW2 PnarbE1, ble*^{R}/poLgaG	This study
potefGFPTub1	*Potef-egfp-tub1, cbx*^{R}	Steinberg *et al.*, 2001
poGLifeact	*Potef-egfp-lifeact, cbx*^{R}	Schuster *et al.*, submitted for publication
poGRab5a	*Potef-egfp-rab5a, nat*^{R}	Schuster *et al.*, 2011(a)
pRFPTub1	*Potef-rfp-tub1, cbx*^{R}	Straube *et al.*, 2005
pKin3G	*Pkin3-kin3-gfp, cbx*^{R}	Wedlich-Söldner *et al.*, 2002(b)
po$_m$ChRab5a	*Potef-mcherry-rab5a, nat*^{R}	Schuster *et al.*, 2011(b)
popaGRab5a	*Potef-pagfp-rab5a, cbx*^{R}	Schuster *et al.*, 2011(a)
poCpYR$_3$	*Potef-cpY-mrfp-mrfp-mrfp, nat*^{R}	J. Schirawski, unpublished
poGSso1	*Potef-egfp-sso1, cbx*^{R}	This study
pERGFP	*Potef-cal*^{s}*-egfp*-HDEL, *cbx*^{R}	Wedlich-Söldner *et al.*, 2002(a)
po$_m$ChTub1	*Potef-mCherry-tub1, cbx*^{R}	Schuster *et al.*, submitted for publication
pGFPYpt1	*Potef-egfp-ypt1, cbx*^{R}	Wedlich-Söldner *et al.*, 2002(a)
pn3GMcs1ΔMM	*Pmcs-3xegfp-mcs1*$^{D57-753}$, *cbx*^{R}	Treitschke *et al.*, 2010
pN_NLS3xRFP	*Potef-gal4s-mrfp-mrfp-mrfp, nat*^{R}	Theisen *et al.*, 2008
pERRFP	*Potef-cal*^{s}*-mrfp*-HDEL, *cbx*^{R}	Theisen *et al.*, 2008
pC_NLS3xRFP	*Potef-gal4s-mrfp-mrfp-mrfp, cbx*^{R}	Straube *et al.*, 2005
pN_ERGFP	*Potef-cal*^{s}*-gfp*-HDEL, *nat*^{R}	Straube *et al.*, 2005
poGSKL	*Potef-egfp*-SKL, *cbx*^{R}	This study
poLgaG	*Potef-lga-egfp, cbx*^{R}	This study

a, *b*, mating type loci; P, promoter; -, fusion; *hyg*R, hygromycin resistance; *ble*R, phleomycin resistance; *nat*R, nourseothricin resistance; *cbx*R, carboxin resistance; Δ, deletion; /, ectopically integrated; *otef*, constitutive promoter; *nar*, conditional nitrate reductase promoter; *E1*, *W2*, genes of the *b* mating type locus; *pagfp*: photo-activatable monomeric green fluorescent protein; *mrfp*, monomeric red fluorescent protein; *mcherry*, monomeric cherry; Tub1, tubulin; Lifeact, first 17 aa of *Abp140*; Myo5: class V myosin; *dyn2*: C-terminal half of the dynein heavy chain; *kin3*, kinesin-3; *rab5a*, small endosomal Rab5-like GTPase; *cpy*, carboxypeptidase Y; *sso1*, a syntaxin-like plasma membrane protein; *calS*, signal sequence of calreticulin from rabbit, HDEL, ER retention signal; *ypt1*, Rab family GTPase; *mcs1*, myosin-chitin synthase 1; *gal4s*, nuclear localisation signal of the GAL-4 DNA binding domain from pC-ACT1 (Clontech); *nup107*, nucleoporin; *egfp*, enhanced green fluorescent protein; SKL, peroxisomal targeting signal; *lga2*, putative mitochondrial matrix protein.

Mitochondria. These organelles were visualised using a fusion of Lga2, which is an *U. maydis*-specific mitochondrial matrix protein (Urban *et al.*, 1996), to eGFP and expressed under the constitutive *otef* promoter. The localisation of Lga2 in mitochondria was shown in (Mahlert *et al.*, 2009).

Growth conditions. Strains were grown in at 28 °C in complete medium (CM) supplemented with 1 % glucose. Hyphal growth in the AB33 background was induced over night by shifting to nitrate minimal medium supplemented with 1 % glucose. This treatment induced the expression of both halves of the *b*-transcription factor and triggered hyphal growth (Brachmann *et al.*, 2001). The Golgi apparatus was visualised in hyphae that were generated by applying mating pheromone. For details on pheromone treatment see (Fuchs *et al.*, 2005).

Microscopy. Cells were placed on a thin layer of 2 % agarose, covered with a cover slip, and observed using a IX81 motorized inverted microscope (Olympus, Hamburg, Germany), equipped with a PlanApo 100X/1.45 Oil TIRF and an UPlanSApo 60X/1.35 Oil objective (Olympus, Hamburg, Germany). Fluorescently-labelled proteins were visualised by using a VS-LMS4 Laser-Merge-System with solid state lasers (488 nm/75 mW and 561 nm/75 mW, Visitron System, Munich, Germany). Images were captured using a Charged-Coupled Device camera (Photometric CoolSNAP HQ2, Roper Scientific, Germany). The software package MetaMorph (Molecular Devices, Downingtown, USA) controls all parts of the system.

Deconvolution and 3D reconstructions. Z-stacks were taken at 200 nm step size with 100 ms exposure time using

Author's personal copy

a Piezo drive (Piezosystem Jena GmbH, Jena, Germany). Z-stacks of all compartments were processed by 10–30 iterations of three-dimensional deconvolution using AutoQuantX software (AutoQuant Imaging, Troy, NY). 3D reconstructions were done using MetaMorph.

Photo-bleaching experiments. Photo-bleaching experiments were performed using a Visitron 2D FRAP system, consisting of a 405 nm/60 mW diode laser which was dimmed by a ND 0.6 Filter, resulting in 15 mW output power. The FRAP laser was controlled by UGA-40 controller (Rapp OptoElectronic GmbH, Hamburg, Germany) and a VisiFRAP 2D FRAP control software for Meta Series 7.5.x (Visitron System, Munich, Germany). Parts of the cells were irradiated by using 100 % output power of the 405 nm laser for 150 ms with a beam diameter of 30 pixels. This was followed by immediate observation. Further details on all methods can be found in (Schuster *et al.*, 2011(a,b)).

Movie conversion. Movie annotation and the generation of video clips in AVI format were done in MetaMorph. Large MOV movies were generated in QuickTime (version 7.6.2, Apple Inc, Cupertino, USA). Small MOV files and MP4 movies were generated using the Leawo Video Converter (Vers. 3.1.0.0, Leawo.com Cooperation; http://www.leawo.com/).

Acknowledgement

The authors wish to thank the following previous lab members for generating plasmids or strains: Dr. Gero Fink (strain AB33paGRab5a_CpYR), Inga Schmid (strain AB33GSso1), Dr. Isabel Schuchardt (strains AB33GSKL, AB33LgaG), Dr. Anne Straube (plasmid poGSKL), and Dr. R. Wedlich-Söldner (poLgaG). Dr. Jan Schirwaski is acknowledged for providing the unpublished plasmid poCpYR$_3$. We wish to thank the Max-Planck-Institute for Terrestrial Microbiology for providing equipment. Our work is supported by the Biotechnology and Biological Science Research Council (BBSRC).

Supplementary material

Supplementary material associated with this article is available, in the online version, at doi:10.1016/j.fbr.2011.01.008.

REFERENCES

Aalto, M.K., Ronne, H., Keränen, S., 1993. Yeast syntaxins Sso1p and Sso2p belong to a family of related membrane proteins that function in vesicular transport. EMBO J. 12, 4095–4104.

Abenza, J.F., Pantazopoulou, A., Rodriguez, J.M., Galindo, A., Penalva, M.A., 2009. Long-distance movement of *Aspergillus nidulans* early endosomes on microtubule tracks. Traffic 10, 57–75.

Abramczyk, D., Park, C., Szaniszlo, P.J., 2009. Cytolocalization of the class V chitin synthase in the yeast, hyphal and sclerotic morphotypes of *Wangiella* (*Exophiala dermatitidis*). Fungal Genet. Biol. 46, 28–41.

Alberti-Segui, C., Dietrich, F., Altmann-Johl, R., Hoepfner, D., Philippsen, P., 2001. Cytoplasmic dynein is required to oppose the force that moves nuclei towards the hyphal tip in the filamentous ascomycete *Ashbya gossypii*. J. Cell Sci. 114, 975–986.

Ashwin, P., Lin, C., Steinberg, G., 2010. Queueing induced by bidirectional motor motion near the end of a microtubule. Phys. Rev. E 82, 1.

Banuett, F., 1995. Genetics of *Ustilago maydis*, a fungal pathogen that induces tumors in maize. Annu. Rev. Genet. 29, 179–208.

Bartnicki-Garcia, S., 2006. Chitosomes: past, present and future. FEMS Yeast Res. 6, 957–965.

Berepiki, A., Lichius, A., Shoji, J.Y., Tilsner, J., Read, N.D., 2010. F-actin dynamics in *Neurospora crassa*. Eukaryot. Cell 9, 547–557.

Bölker, M., 2001. *Ustilago maydis* – a valuable model system for the study of fungal dimorphism and virulence. Microbiology 147, 1395–1401.

Brachmann, A., Weinzierl, G., Kamper, J., Kahmann, R., 2001. Identification of genes in the bW/bE regulatory cascade in *Ustilago maydis*. Mol. Microbiol. 42, 1047–1063.

Brand, A., Gow, N.A., 2009. Mechanisms of hypha orientation of fungi. Curr. Opin. Microbiol. 12, 350–357.

Brefort, T., Doehlemann, G., Mendoza-Mendoza, A., Reissmann, S., Djamei, A., Kahmann, R., 2009. *Ustilago maydis* as a pathogen. Annu. Rev. Phytopathol. 47, 423–445.

Bristowe, J.S., 1854. Vegetable fungus growing in a cavity of a lung. Trans. Pathol. Soc. London 5, 38–41.

Brunswik, H., 1924. Untersuchungen über die Geschlechts- und Kernverhältnisse bei der Hymenomyzetengattung *Coprinus*. Bot. Abh. 5, 1–152.

Canovas, D., Perez-Martin, J., 2009. Sphingolipid biosynthesis is required for polar growth in the dimorphic phytopathogen *Ustilago maydis*. Fungal Genet. Biol. 46, 190–200.

Capelson, M., Hetzer, M.W., 2009. The role of nuclear pores in gene regulation, development and disease. EMBO Rep. 10, 697–705.

Carminati, J.L., Stearns, T., 1997. Microtubules orient the mitotic spindle in yeast through dynein-dependent interactions with the cell cortex. J. Cell Biol. 138, 629–641.

Darrah, P.R., Tlalka, M., Ashford, A., Watkinson, S.C., Fricker, M.D., 2006. The vacuole system is a significant intracellular pathway for longitudinal solute transport in basidiomycete fungi. Eukaryot. Cell 5, 1111–1125.

De Souza, C.P., Osmani, A.H., Hashmi, S.B., Osmani, S.A., 2004. Partial nuclear pore complex disassembly during closed mitosis in *Aspergillus nidulans*. Curr. Biol. 14, 1973–1984.

De Souza, C.P., Osmani, S.A., 2007. Mitosis, not just open or closed. Eukaryot. Cell 6, 1521–1527.

Delgado-Alvarez, D.L., Callejas-Negrete, O.A., Gomez, N., Freitag, M., Roberson, R.W., Smith, L.G., Mourino-Perez, R.R., 2010. Visualization of F-actin localization and dynamics with live cell markers in *Neurospora crassa*. Fungal Genet. Biol. 47, 573–586.

Ding, D.Q., Chikashige, Y., Haraguchi, T., Hiraoka, Y., 1998. Oscillatory nuclear movement in fission yeast meiotic prophase is driven by astral microtubules, as revealed by continuous observation of chromosomes and microtubules in living cells. J. Cell Sci. 111, 701–712.

Fink, G., Schuchardt, I., Colombelli, J., Stelzer, E., Steinberg, G., 2006. Dynein-mediated pulling forces drive rapid mitotic spindle elongation in *Ustilago maydis*. EMBO J. 25, 4897–4908.

Fink, G., Steinberg, G., 2006. Dynein-dependent motility of microtubules and nucleation sites supports polarization of the tubulin array in the fungus *Ustilago maydis*. Mol. Biol. Cell 17, 3242–3253.

Fischer, R., Zekert, N., Takeshita, N., 2008. Polarized growth in fungi-interplay between the cytoskeleton, positional markers and membrane domains. Mol. Microbiol. 68, 813–826.

Fricker, M.D., Lee, J.A., Bebber, D.P., Tlalka, M., Hynes, J., Darrah, P.R., Watkinson, S.C., Boddy, L., 2008. Imaging complex nutrient dynamics in mycelial networks. J. Microsc. 231, 317–331.

Fuchs, F., Westermann, B., 2005. Role of Unc104/KIF1-related motor proteins in mitochondrial transport in *Neurospora crassa*. Mol. Biol. Cell 16, 153–161.

Author's personal copy

Fuchs, U., Manns, I., Steinberg, G., 2005. Microtubules are dispensable for the initial pathogenic development but required for long-distance hyphal growth in the corn smut fungus *Ustilago maydis*. Mol. Biol. Cell 16, 2746–2758.

Fuchs, U., Hause, G., Schuchardt, I., Steinberg, G., 2006. Endocytosis is essential for pathogenic development in the corn smut fungus *Ustilago maydis*. Plant Cell 18, 2066–2081.

Fujiwara, M., Horiuchi, H., Ohta, A., Takagi, M., 1997. A novel fungal gene encoding chitin synthase with a myosin motor-like domain. Biochem. Biophys. Res. Commun. 236, 75–78.

Gladfelter, A.S., 2010. Guides to the final frontier of the cytoskeleton: septins in filamentous fungi. Curr. Opin. Microbiol. 13, 720–726.

Hallmann, J., Quadt-Hallmann, A., Deml, G., 2010. Julius Kühn und die Kulturpflanzen: Ein historischer Überblick seiner Arbeiten anlässlich des 100sten Todestages. Journal für Kulkturpflanzen 62, 125–141.

Han, G., Liu, B., Zhang, J., Zuo, W., Morris, N.R., Xiang, X., 2001. The *Aspergillus* cytoplasmic dynein heavy chain and NUDF localize to microtubule ends and affect microtubule dynamics. Curr. Biol. 11, 719–724.

Harris, S.D., Read, N.D., Roberson, R.W., Shaw, B., Seiler, S., Plamann, M., Momany, M., 2005. Polarisome meets Spitzenkörper: microscopy, genetics, and genomics converge. Eukaryot. Cell 4, 225–229.

Heath, I.B., 1995. The cytoskeleton. In: Gow, N.A.R., Gadd, G.M. (Eds), The Growing Fungus. Chapman and Hall, London.

Heath, I.B., Steinberg, G., 1999. Mechanisms of hyphal tip growth: tube dwelling amebae revisited. Fungal Genet. Biol. 28, 79–93.

Heath, I.B., Gupta, G., Bai, S., 2000. Plasma membrane-adjacent actin filaments, but not microtubules, are essential for both polarization and hyphal tip morphogenesis in *Saprolegnia ferax* and *Neurospora crassa*. Fungal Genet. Biol. 30, 45–62.

Hinson, K.F.W., Moon, A.J., Plummer, N.S., 1952. Bronchopulmonary aspergillosis. Thorax 7, 317–333.

Hooke, R., 1665. Micrographia: or Some Physiological Descriptions of Minute Bodies Made by Magnifying Glasses with Observations and Inquiries There Upon. Royal Society, London.

Horio, T., Oakley, B.R., 2005. The role of microtubules in rapid hyphal tip growth of *Aspergillus nidulans*. Mol. Biol. Cell 16, 918–926.

Idnurm, A., Giles, S.S., Perfect, J.R., Heitman, J., 2007. Peroxisome function regulates growth on glucose in the basidiomycete fungus *Cryptococcus neoformans*. Eukaryot. Cell 6, 60–72.

Imazaki, A., Tanaka, A., Harimoto, Y., Yamamoto, M., Akimitsu, K., Park, P., Tsuge, T., 2010. Contribution of peroxisomes to secondary metabolism and pathogenicity in the fungal plant pathogen *Alternaria alternata*. Eukaryot. Cell 9, 682–694.

Kahmann, R., Romeis, T., Bolker, M., Kämper, J., 1995. Control of mating and development in *Ustilago maydis*. Curr. Opin. Genet. Dev. 5, 559–564.

Kaksonen, M., Sun, Y., Drubin, D.G., 2003. A pathway for association of receptors, adaptors, and actin during endocytic internalization. Cell 115, 475–487.

Kamena, F., Diefenbacher, M., Kilchert, C., Schwarz, H., Spang, A., 2008. Ypt1p is essential for retrograde Golgi–ER transport and for Golgi maintenance in *S. cerevisiae*. J. Cell Sci. 121, 1293–1302.

Kämper, J., Reichmann, M., Romeis, T., Bölker, M., Kahmann, R., 1995. Multiallelic recognition: nonself-dependent dimerization of the bE and bW homeodomain proteins in *Ustilago maydis*. Cell 81, 73–83.

Kiel, J.A., Hilbrands, R.E., Bovenberg, R.A., Veenhuis, M., 2000. Isolation of *Penicillium chrysogenum* PEX1 and PEX6 encoding AAA proteins involved in peroxisome biogenesis. Appl. Microbiol. Biotechnol. 54, 238–242.

Kim, K.Y., Truman, A.W., Caesar, S., Schlenstedt, G., Levin, D.E., 2010. Yeast Mpk1 cell wall integrity mitogen-activated protein kinase regulates nucleocytoplasmic shuttling of the Swi6 transcriptional regulator. Mol. Biol. Cell 21, 1609–1619.

Klionsky, D.J., Herman, P.K., Emr, S.D., 1990. The fungal vacuole: composition, function, and biogenesis. Microbiol. Rev. 54, 266–292.

Konzack, S., Rischitor, P.E., Enke, C., Fischer, R., 2005. The role of the kinesin motor KipA in microtubule organization and polarized growth of *Aspergillus nidulans*. Mol. Biol. Cell 16, 497–506.

Kühn, J., 1858. Die Krankheiten der Kulturgewächse, ihre Ursachen und ihre Verhütung. Gustav Bosselmann, Berlin.

Lange, A., Mills, R.E., Lange, C.J., Stewart, M., Devine, S.E., Corbett, A.H., 2007. Classical nuclear localization signals: definition, function, and interaction with importin alpha. J. Biol. Chem. 282, 5101–5105.

Latge, J.P., 2007. The cell wall: a carbohydrate armour for the fungal cell. Mol. Microbiol. 66, 279–290.

Lenz, J.H., Schuchardt, I., Straube, A., Steinberg, G., 2006. A dynein loading zone for retrograde endosome motility at microtubule plus-ends. EMBO J. 25, 2275–2286.

Lewin, A.S., Hines, V., Small, G.M., 1990. Citrate synthase encoded by the CIT2 gene of *Saccharomyces cerevisiae* is peroxisomal. Mol. Cell Biol. 10, 1399–1405.

Madrid, M.P., Di Pietro, A., Roncero, M.I., 2003. Class V chitin synthase determines pathogenesis in the vascular wilt fungus *Fusarium oxysporum* and mediates resistance to plant defence compounds. Mol. Microbiol. 47, 257–266.

Maerz, S., Seiler, S., 2010. Tales of RAM and MOR: NDR kinase signaling in fungal morphogenesis. Curr. Opin. Microbiol. 13, 663–671.

Mahlert, M., Vogler, C., Stelter, K., Hause, G., Basse, C.W., 2009. The a2 mating-type-locus gene lga2 of *Ustilago maydis* interferes with mitochondrial dynamics and fusion, partially in dependence on a Dnm1-like fission component. J. Cell Sci. 122, 2402–2412.

Martin, R., Walther, A., Wendland, J., 2004. Deletion of the dynein heavy-chain gene DYN1 leads to aberrant nuclear positioning and defective hyphal development in *Candida albicans*. Eukaryot. Cell 3, 1574–1588.

Martin, S.W., Konopka, J.B., 2004. Lipid raft polarization contributes to hyphal growth in *Candida albicans*. Eukaryot. Cell 3, 675–684.

Mehrabi, R., Bahkali, A.H., Abd-Elsalam, K.A., Moslem, M., Ben M'barek, S., Gohari, A.M., Jashni, M.K., Stergiopoulos, I., Kema, G.H., de Wit, P.J., 2011. Horizontal gene and chromosome transfer in plant pathogenic fungi affecting host range. FEMS Microbiol., (Epub ahead of print).

Nielsen, K., Heitman, J., 2007. Sex and virulence of human pathogenic fungi. Adv. Genet. 57, 143–173.

Oakley, B.R., 2004. Tubulins in *Aspergillus nidulans*. Fungal Genet. Biol. 41, 420–427.

Ohneda, M., Arioka, M., Nakajima, H., Kitamoto, K., 2002. Visualization of vacuoles in *Aspergillus oryzae* by expression of CPY-EGFP. Fungal Genet. Biol. 37, 29–38.

Osmani, A.H., Davies, J., Liu, H.L., Nile, A., Osmani, S.A., 2006. Systematic deletion and mitotic localization of the nuclear pore complex proteins of *Aspergillus nidulans*. Mol. Biol. Cell 17, 4946–4961.

Penalva, M.A., 2010. Endocytosis in filamentous fungi: Cinderella gets her reward. Curr. Opin. Microbiol. 13, 684–692.

Perez-Martin, J., Castillo-Lluva, S., Sgarlata, C., Flor-Parra, I., Mielnichuk, N., Torreblanca, J., Carbo, N., 2006. Pathocycles: *Ustilago maydis* as a model to study the relationships between cell cycle and virulence in pathogenic fungi. Mol. Genet. Genomics 276, 211–229.

Plamann, M., Minke, P.F., Tinsley, J.H., Bruno, K.S., 1994. Cytoplasmic dynein and actin-related protein Arp1 are required for normal nuclear distribution in filamentous fungi. J. Cell Sci. 127, 139–149.

Author's personal copy

Preuss, D., Mulholland, J., Franzusoff, A., Segev, N., Botstein, D., 1992. Characterization of the *Saccharomyces* Golgi complex through the cell cycle by immunoelectron microscopy. Mol. Biol. Cell 3, 789–803.

Read, N.D., Lichius, A., Shoji, J.Y., Goryachev, A.B., 2009. Self-signalling and self-fusion in filamentous fungi. Curr. Opin. Microbiol. 12, 608–615.

Reinhardt, M.O., 1892. Das Wachsthum der Pilzhyphen. Jahrb. Wissenschaft. Bot. 23, 479–566.

Riedl, J., Crevenna, A.H., Kessenbrock, K., Yu, J.H., Neukirchen, D., Bista, M., Bradke, F., Jenne, D., Holak, T.A., Werb, Z., Sixt, M., Wedlich-Söldner, R., 2008. Lifeact: a versatile marker to visualize F-actin. Nat. Methods 5, 605–607.

Riquelme, M., Bartnicki-Garcia, S., Gonzalez-Prieto, J.M., Sanchez-Leon, E., Verdin-Ramos, J.A., Beltran-Aguilar, A., Freitag, M., 2007. Spitzenkörper localization and intracellular traffic of green fluorescent protein-labeled CHS-3 and CHS-6 chitin synthases in living hyphae of *Neurospora crassa*. Eukaryot. Cell 6, 1853–1864.

Rodal, A.A., Kozubowski, L., Goode, B.L., Drubin, D.G., Hartwig, J.H., 2005. Actin and septin ultrastructures at the budding yeast cell cortex. Mol. Biol. Cell 16, 372–384.

Schrader, M., Fahimi, H.D., 2008. The peroxisome: still a mysterious organelle. Histochem. Cell Biol. 129, 421–440.

Schuchardt, I., Assmann, D., Thines, E., Schuberth, C., Steinberg, G., 2005. Myosin-V, Kinesin-1, and Kinesin-3 cooperate in hyphal growth of the fungus *Ustilago maydis*. Mol. Biol. Cell 16, 5191–5201.

Schulz, B., Banuett, F., Dahl, M., Schlesinger, R., Schafer, W., Martin, T., Herskowitz, I., Kahmann, R., 1990. The b alleles of *U. maydis*, whose combinations program pathogenic development, code for polypeptides containing a homeodomain-related motif. Cell 60, 295–306.

Schuster, M., Kilaru, S., Ashwin, P., Congping, L., Severs, N.J., Steinberg, G., 2011. Controlled and stochastic retention concentrates dynein at microtubule ends to keep endosomes on track. EMBO J., (Epub ahead of print)(a).

Schuster, M., Lipowsky, R., Assmann, M.A., Lenz, P., Steinberg, G, 2011. Transient binding of dynein controls bidirectional long-range motility of early endosomes. Proc. Natl. Acad. Sci. USA, (Epub ahead of print)(b).

Segev, N., Mulholland, J., Botstein, D., 1988. The yeast GTP-binding YPT1 protein and a mammalian counterpart are associated with the secretion machinery. Cell 52, 915–924.

Seider, K., Heyken, A., Luttich, A., Miramon, P., Hube, B., 2010. Interaction of pathogenic yeasts with phagocytes: survival, persistence and escape. Curr. Opin. Microbiol. 13, 392–400.

Sietsma, J.H., Beth Din, A., Ziv, V., Sjollema, K.A., Yarden, O., 1996. The localization of chitin synthase in membranous vesicles (chitosomes) in *Neurospora crassa*. Microbiology 142, 1591–1596.

Singer, S.J., Nicolson, G.L., 1972. The fluid mosaic model of the structure of cell membranes. Science 175, 720–731.

Skamnioti, P., Gurr, S.J., 2009. Against the grain: safeguarding rice from rice blast disease. Trends Biotechnol. 27, 141–150.

Spellig, T., Bölker, M., Lottspeich, F., Frank, R.W., Kahmann, R., 1994. Pheromones trigger filamentous growth in *Ustilago maydis*. EMBO J. 13, 1620–1627.

Sprote, P., Brakhage, A.A., Hynes, M.J., 2009. Contribution of peroxisomes to penicillin biosynthesis in *Aspergillus nidulans*. Eukaryot. Cell 8, 421–423.

Steinberg, G., 2007a. Hyphal growth: a tale of motors, lipids, and the Spitzenkörper. Eukaryot. Cell 6, 351–360.

Steinberg, G., 2007b. On the move: endosomes in fungal growth and pathogenicity. Nat. Rev. Microbiol. 5, 309–316.

Steinberg, G., Wedlich-Söldner, R., Brill, M., Schulz, I., 2001. Microtubules in the fungal pathogen *Ustilago maydis* are highly dynamic and determine cell polarity. J. Cell Sci. 114, 609–622.

Steinberg, G., Perez-Martin, J., 2008. *Ustilago maydis*, a new fungal model system for cell biology. Trends Cell Biol. 18, 61–67.

Straube, A., Brill, M., Oakley, B.R., Horio, T., Steinberg, G., 2003. Microtubule organization requires cell cycle-dependent nucleation at dispersed cytoplasmic sites: polar and perinuclear microtubule organizing centers in the plant pathogen *Ustilago maydis*. Mol. Biol. Cell 14, 642–657.

Straube, A., Enard, W., Berner, A., Wedlich-Söldner, R., Kahmann, R., Steinberg, G., 2001. A split motor domain in a cytoplasmic dynein. EMBO J. 20, 5091–5100.

Straube, A., Weber, I., Steinberg, G., 2005. A novel mechanism of nuclear envelope break-down in a fungus: nuclear migration strips off the envelope. EMBO J. 24, 1674–1685.

Su, W., Li, S., Oakley, B.R., Xiang, X., 2004. Dual-color imaging of nuclear division and mitotic spindle elongation in live cells of *Aspergillus nidulans*. Eukaryot. Cell 3, 553–556.

Sudbery, P., Gow, N., Berman, J., 2004. The distinct morphogenic states of *Candida albicans*. Trends Microbiol. 12, 317–324.

Theisen, U., Straube, A., Steinberg, G., 2008. Dynamic rearrangement of nucleoporins during fungal "open" mitosis. Mol. Biol. Cell 19, 1230–1240.

Treitschke, S., Doehlemann, G., Schuster, M., Steinberg, G., 2010. The myosin motor domain of fungal chitin synthase V is dispensable for vesicle motility but required for virulence of the maize pathogen *Ustilago maydis*. Plant Cell 22, 2476–2494.

Urban, M., Kahmann, R., Bölker, M., 1996. The biallelic a mating type locus of *Ustilago maydis*: remnants of an additional pheromone gene indicate evolution from a multiallelic ancestor. Mol. Gen. Genet. 250, 414–420.

Vale, R.D., 2003. The molecular motor toolbox for intracellular transport. Cell 112, 467–480.

Valenciano, S., De Lucas, J.R., Van der Klei, I., Veenhuis, M., Laborda, F., 1998. Characterization of *Aspergillus nidulans* peroxisomes by immunoelectron microscopy. Arch. Microbiol. 170, 370–376.

van de Veerdonk, F.L., Kullberg, B.J., van der Meer, J.W., Gow, N.A., Netea, M.G., 2008. Host–microbe interactions: innate pattern recognition of fungal pathogens. Curr. Opin. Microbiol. 11, 305–312.

van der Klei, I., Veenhuis, M., 2002. Peroxisomes: flexible and dynamic organelles. Curr. Opin. Cell Biol. 14, 500–505.

Vauchelles, R., Stalder, D., Botton, T., Arkowitz, R.A., Bassilana, M., 2010. Rac1 dynamics in the human opportunistic fungal pathogen *Candida albicans*. PloS ONE 5, e15400.

Veses, V., Richards, A., Gow, N.A., 2008. Vacuoles and fungal biology. Curr. Opin. Microbiol. 11, 503–510.

Weber, I., Assmann, D., Thines, E., Steinberg, G., 2006. Polar localizing class V myosin chitin synthases are essential during early plant infection in the plant pathogenic fungus *Ustilago maydis*. Plant Cell 18, 225–242.

Weber, I., Gruber, C., Steinberg, G., 2003. A class-V myosin required for mating, hyphal growth, and pathogenicity in the dimorphic plant pathogen *Ustilago maydis*. Plant Cell 15, 2826–2842.

Wedlich-Söldner, R., Straube, A., Friedrich, M.W., Steinberg, G., 2002a. A balance of KIF1A-like kinesin and dynein organizes early endosomes in the fungus *Ustilago maydis*. EMBO J. 21, 2946–2957.

Wedlich-Söldner, R., Schulz, I., Straube, A., Steinberg, G., 2002b. Dynein supports motility of endoplasmic reticulum in the fungus *Ustilago maydis*. Mol. Biol. Cell 13, 965–977.

Westermann, B., Prokisch, H., 2002. Mitochondrial dynamics in filamentous fungi. Fungal Genet. Biol. 36, 91–97.

Wilson, R.A., Talbot, N.J., 2009. Under pressure: investigating the biology of plant infection by *Magnaporthe oryzae*. Nat. Rev. Microbiol. 7, 185–195.

Author's personal copy

Woo, M., Lee, K., Song, K., 2003. MYO2 is not essential for viability, but is required for polarized growth and dimorphic switches in *Candida albicans*. FEMS Microbiol. Lett. 218, 195–202.

Xiang, X., Fischer, R., 2004. Nuclear migration and positioning in filamentous fungi. Fungal Genet. Biol. 41, 411–419.

Xiang, X., Plamann, M., 2003. Cytoskeleton and motor proteins in filamentous fungi. Curr. Opin. Microbiol. 6, 628–633.

Xiang, X., Beckwith, S.M., Morris, N.R., 1994. Cytoplasmic dynein is involved in nuclear migration in *Aspergillus nidulans*. Proc. Natl. Acad. Sci. USA 91, 2100–2104.

Zarnack, K., Feldbrügge, M., 2010. Microtubule-dependent mRNA transport in fungi. Eukaryot. Cell 9, 982–990.

Zekert, N., Fischer, R., 2009. The *Aspergillus nidulans* kinesin-3 UncA motor moves vesicles along a subpopulation of microtubules. Mol. Biol. Cell 20, 673–684.

Zekert, N., Veith, D., Fischer, R., 2010. Interaction of the *Aspergillus nidulans* microtubule-organizing center (MTOC) component ApsB with gamma-tubulin and evidence for a role of a subclass of peroxisomes in the formation of septal MTOCs. Eukaryot. Cell 9, 795–805.

Zhang, J., Zhuang, L., Lee, Y., Abenza, J.F., Penalva, M.A., Xiang, X., 2010. The microtubule plus-end localization of *Aspergillus* dynein is important for dynein-early-endosome interaction but not for dynein ATPase activation. J. Cell Sci. 123, 3596–3604.

Zhang, J., Li, S., Fischer, R., Xiang, X., 2003. Accumulation of cytoplasmic dynein and dynactin at microtubule plus ends in *Aspergillus nidulans* is kinesin dependent. Mol. Biol. Cell 14, 1479–1488.

Zhuang, X., Tlalka, M., Davies, D.S., Allaway, W.G., Watkinson, S.C., Ashford, A.E., 2009. Spitzenkörper, vacuoles, ring-like structures, and mitochondria of *Phanerochaete velutina* hyphal tips visualized with carboxy-DFFDA, CMAC and DiOC6(3). Mycol. Res. 113, 417–431.